



**HAL**  
open science

# Towards the modeling of the interplay between radiation induced segregation and sink microstructure

Thomas Schuler, Maylise Nastar, Frédéric Soisson

## ► To cite this version:

Thomas Schuler, Maylise Nastar, Frédéric Soisson. Towards the modeling of the interplay between radiation induced segregation and sink microstructure. *Journal of Applied Physics*, 2022, 132, pp.080903. 10.1063/5.0100298 . cea-03775668

**HAL Id: cea-03775668**

**<https://cea.hal.science/cea-03775668>**

Submitted on 12 Sep 2022

**HAL** is a multi-disciplinary open access archive for the deposit and dissemination of scientific research documents, whether they are published or not. The documents may come from teaching and research institutions in France or abroad, or from public or private research centers.

L'archive ouverte pluridisciplinaire **HAL**, est destinée au dépôt et à la diffusion de documents scientifiques de niveau recherche, publiés ou non, émanant des établissements d'enseignement et de recherche français ou étrangers, des laboratoires publics ou privés.

# Towards the modeling of the interplay between radiation induced segregation and sink microstructure

Cite as: J. Appl. Phys. **132**, 080903 (2022); <https://doi.org/10.1063/5.0100298>

Submitted: 23 May 2022 • Accepted: 05 August 2022 • Published Online: 31 August 2022

T. Schuler,  M. Nastar and  F. Soisson

## COLLECTIONS

Paper published as part of the special topic on [Radiation Effects in Materials](#)

 This paper was selected as an Editor's Pick



View Online



Export Citation



CrossMark

## ARTICLES YOU MAY BE INTERESTED IN

[The impact of rapid thermal annealing for the ferroelectricity of undoped sputtered HfO<sub>2</sub> and its wake-up effect](#)

Journal of Applied Physics **132**, 094101 (2022); <https://doi.org/10.1063/5.0100562>

[Impact of charge character on anionic cyanine-based organic salt photovoltaics](#)

Journal of Applied Physics **132**, 085501 (2022); <https://doi.org/10.1063/5.0104901>

[An innovative wide and low-frequency bandgap metastructure for vibration isolation](#)

Journal of Applied Physics **132**, 084903 (2022); <https://doi.org/10.1063/5.0102410>





## Instruments for Advanced Science

- Knowledge,
- Experience,
- Expertise

Click to view our product catalogue

Contact Hiden Analytical for further details:  
[www.HidenAnalytical.com](http://www.HidenAnalytical.com)  
[info@hideninc.com](mailto:info@hideninc.com)

Gas Analysis



- ▶ dynamic measurement of reaction gas streams
- ▶ catalysis and thermal analysis
- ▶ molecular beam studies
- ▶ dissolved species probes
- ▶ fermentation, environmental and ecological studies

Surface Science



- ▶ UHVTPD
- ▶ SIMS
- ▶ end point detection in ion beam etch
- ▶ elemental imaging - surface mapping

Plasma Diagnostics



- ▶ plasma source characterization
- ▶ etch and deposition process reaction kinetic studies
- ▶ analysis of neutral and radical species

Vacuum Analysis



- ▶ partial pressure measurement and control of process gases
- ▶ reactive sputter process control
- ▶ vacuum diagnostics
- ▶ vacuum coating process monitoring

# Towards the modeling of the interplay between radiation induced segregation and sink microstructure



Cite as: J. Appl. Phys. **132**, 080903 (2022); doi: [10.1063/5.0100298](https://doi.org/10.1063/5.0100298)

Submitted: 23 May 2022 · Accepted: 5 August 2022 ·

Published Online: 31 August 2022



View Online



Export Citation



CrossMark

T. Schuler, M. Nastar, and F. Soisson<sup>a)</sup>

## AFFILIATIONS

Service de Recherches de Métallurgie Physique, Université Paris-Saclay, CEA, 91191 Gif-sur-Yvette, France

**Note:** This paper is part of the Special Topic on Radiation Effects in Materials.

<sup>a)</sup>Author to whom correspondence should be addressed: [frederic.soisson@cea.fr](mailto:frederic.soisson@cea.fr)

## ABSTRACT

Excess point defects created by irradiation in metallic alloys diffuse and annihilate at sinks available in the microstructure, such as grain boundaries, dislocations, or point defect clusters. Fluxes of defects create fluxes of alloying elements, leading to local changes of composition near the sinks and to a modification of the properties of the materials. The direction and the amplitude of this radiation-induced segregation, its tendency to produce an enrichment or a depletion of solute, depend on a set of transport coefficients that are very difficult to measure experimentally. The understanding of radiation-induced segregation phenomena has, however, made significant progress in recent years, thanks to the modeling at different scales of diffusion and segregation mechanisms. We review here these different advances and try to identify the key scientific issues that limit the development of predictive models, applicable to real alloys. The review addresses three main issues: the calculation of the transport coefficients from *ab initio* calculations, the modeling of segregation kinetics at static point defects sinks—mainly by kinetic Monte Carlo or diffusion-reaction models—and the more challenging task of modeling the dynamic interplay between radiation-induced segregation and sink microstructure evolution, especially when this evolution results from annihilation of point defects. From this overview of the current state-of-the-art in this field, we discuss still-open questions and guidelines for what constitutes, in our opinion, the desirable future works on this topic.

Published under an exclusive license by AIP Publishing. <https://doi.org/10.1063/5.0100298>

## I. INTRODUCTION

Irradiation creates an excess of point defects (PDs) in materials, which results in a thermodynamic force to eliminate them and recover the equilibrium PD concentrations. The continuous production and elimination of PDs (vacancies and self-interstitial atoms) is at the heart of a whole variety of phenomena<sup>1,2</sup> specific to irradiated materials that cause microstructure evolution and chemical redistribution and, therefore, affects the material's properties over time. Radiation-induced segregation (RIS) is one of such phenomena, which was anticipated by the pioneering works of Anthony<sup>3</sup> and first observed experimentally by Okamoto *et al.*<sup>4</sup> RIS has important technological consequences in the nuclear industry.<sup>2</sup> In austenitic steels, widely used for structures supporting the nuclear core of light water reactors, it usually leads to a depletion of Cr and an enrichment of Ni at grain boundaries and potentially

to a lower resistance to intergranular corrosion and stress corrosion cracking. In ferritic steels, which are considered as interesting candidates for future fission and fusion reactors, RIS is known to produce a segregation of interstitial impurities such as P, with significant consequences for grain boundary embrittlement. Enrichment and depletion of Cr are also observed, but they are less systematic and less well understood than in austenitic steels.

The experimental quantification of RIS poses technical difficulties, even though there has been tremendous progress over the last decade, especially with the advancement regarding atom-probe tomography measurements.<sup>5–8</sup> One of the main difficulties—not only related to RIS but to the general study of materials behavior under irradiation—is the ability to obtain and study neutron-irradiated samples. The vast majority of experimental studies on irradiation, therefore, emulate the effect of neutrons by other irradiation particles (electrons, protons, and ions). The issue

is that the irradiation fluxes with charged particles are orders of magnitude higher than those experienced by materials in a nuclear power plant environment. Drawing solid conclusions from these substitution experiments requires a comprehensive understanding of all the microscopic mechanisms involved,<sup>9</sup> hence the need for rigorous models of irradiation-induced phenomena, and this review focuses on the modeling of RIS.

In the Onsager formulation of irreversible processes,<sup>10,11</sup> fluxes of atoms are expressed as

$$\mathbf{J}_\beta = - \sum_\alpha L_{\beta\alpha} \frac{\nabla\mu_\alpha}{k_B T} - \sum_d L_{\beta d} \frac{\nabla\mu_d}{k_B T}, \quad (1)$$

where  $\alpha$  and  $\beta$  represent chemical species while  $d$  represents PDs, i.e., vacancies (V) and self-interstitial atoms (SIA). The gradients of chemical potential,  $\nabla\mu_\alpha$ , are the thermodynamic driving forces and the  $L_{\beta\alpha}$  and  $L_{\beta d}$  variables represent the transport coefficients.

If we assume that prior to irradiation the material is at equilibrium, all the chemical potentials are homogeneous and therefore there are not net fluxes in the system. Irradiation creates a supersaturation of PDs. These PDs are able to eliminate at various locations of the material where a lattice discontinuity occurs (grain boundaries, dislocations, surfaces, and precipitate/matrix interfaces), which are called PD sinks. At these locations, it is assumed that PDs are at equilibrium, and therefore, the supersaturation of PDs created by irradiation entails non-homogeneous PD chemical potentials, which itself results in fluxes, not only defect fluxes but also fluxes of chemical species. This is captured by the  $L_{\alpha d}$  coefficients of Eq. (1) from which the RIS phenomenon emerges. A first question to ask is: how can we obtain the values of transport coefficients?

The time evolution of the PD chemical potentials (i.e., the driving force) results from the competition between the rate of creation of PDs by irradiation and their ability to migrate toward sinks to eliminate. Eventually, the system will reach a quasi-steady state with concentration profiles of chemical species and PDs that are constant over periods of time where the sink microstructure evolves slowly. For a given chemical species, the difference between this concentration profile and the equilibrium one quantifies the RIS phenomenon.

As we shall see, there are various techniques to solve the quasi-stationary PD concentration for given irradiation conditions. The most simple one relies on a mean field rate theory model that treats PD clustering and elimination at sinks as homogeneous reactions,<sup>12</sup> i.e., diffusion equations are not treated explicitly. In this very efficient model that is at the root of cluster dynamics simulations, the atomic fraction ( $X_d$ ) of PD  $d$  is assumed to be controlled by three reactions: the production rate of Frenkel pairs, the mutual recombination between SIA and vacancy, and the elimination of PDs at sinks,

$$\frac{dX_d}{dt} = G - K_R X_V X_I - k_d^2 D_d (X_d - X_d^{\text{eq}}), \quad d = \text{V or I}, \quad (2)$$

where  $G$  is the radiation dose rate in units of displacement per atom per second (dpa/s).  $K_R = (4\pi R_c / \Omega)(D_I + D_V)$  stands for the SIA-vacancy recombination rate, with  $\Omega$  being the atomic

volume.  $R_c$  is the SIA-vacancy recombination radius, usually assumed to be a few lattice parameters.  $D_d$  is the diffusion coefficient of PD  $d$  and  $X_d^{\text{eq}}$  is the PD atomic fraction at equilibrium.  $k_d^2$  is the sink strength for PD  $d$ , related to the sink density and efficiency in absorbing defect  $d$ . At this scale, PD sinks are usually assumed to be neutral (i.e., any sink bias is neglected), hence  $k_V^2 = k_I^2 = k^2$ . Note that  $k^2 = \sum_s k_s^2$  is the total sink strength, which is summed up over all contributions of the various PD sinks ( $k_s^2$ ). As long as we neglect the mobility of PD clusters, we can assume that atomic diffusion linearly increases with the PD concentration, a phenomenon denoted as Radiation Enhanced Diffusion (RED). Therefore, such a rate theory model provides a first estimation of RED.

The tendency for a given chemical species to be enriched or depleted at a given sink is controlled by transport coefficients, and it does not depend on the structure and properties of the sink itself, but the magnitude and shape of the segregation profile does. The above-mentioned rate theory model is homogeneous and, therefore, not spatially resolved. To quantify RIS around a given sink, one must explicitly solve diffusion equations [Eq. (1)] in conjunction with PD production and recombination reactions. Practically speaking, the last term in Eq. (2) must be replaced by an explicit diffusion term,

$$\frac{dX_d}{dt} = G - K_R X_V X_I - \nabla \cdot \mathbf{J}_d, \quad d = \text{V or I}, \quad (3)$$

where the flux of PD  $d$  is given by Eq. (1). Note that contrary to Eq. (2), all the involved quantities are spatially dependent on Eq. (3). Such reaction–diffusion equations are usually solved by numerical integration (e.g., finite differences or more sophisticated approaches). The second question we want to address is: what tools are available to quantify RIS for a given sink and how good are they?

The ability of PDs to eliminate at sinks depends on the microstructure (density, geometry, and efficiency of locally available sinks) as well as the material (local concentration of chemical species interacting with the PD on its way to the sink), and both are evolving in the course of irradiation. The most prominent example of microstructure evolution is the fact that PD clusters are themselves PD sinks and by definition they will grow in size by absorbing PDs, which will affect their ability to eliminate other PDs later on. In the above, it was implicitly assumed that the sink strength was constant. Yet, the evolving microstructure introduces another timescale, in addition to those of PD and alloying elements diffusion. It is not always obvious to justify that these timescales are well separated and that it is correct to assume that PDs and solutes are always diffusing in a quasi-steady state sink microstructure because the elimination and creation of PDs locally accommodate the number of lattice sites, and therefore, the same physical mechanism responsible for RIS also affects the local structure—and therefore the sink strength—of PD sinks. Of course, extended defects are usually subjected to other evolution mechanisms (e.g., driven by local stresses) and topologically constrained. This brings us to a third question: are we able to account for the time and space dependence of the RIS phenomenon in conjunction with the dynamic character of the sink microstructure?

There have been recent and comprehensive reviews on RIS,<sup>13,14</sup> and therefore, this paper focuses on some of the most recent studies related to the modeling of RIS as well as the authors' views on still open questions and the desired evolution of the field in the near future. Most of the available studies on RIS are related to metallic alloys and we shall confine our discussion to those, even though RIS also occurs in other materials, e.g., in ceramics.<sup>15</sup> In such case, the additional complexity of defect charges (PDs and extended defects) introduces an extra layer of complexity due to electro-migration.<sup>16</sup>

The previous paragraphs and the associated questions naturally lead to the outline of this paper. Section II will provide details about the calculation of transport coefficients from atomic-scale data; Sec. III will give an overview of various methods available to model RIS around a particular sink; and Sec. IV will discuss the challenges associated with coupling the methods from Secs. II and III with the time-evolution of the irradiated microstructure. RIS being intrinsically a multi-scale phenomenon, each one of these sections operates at different scales. In the final part of the paper (Sec. V), we will discuss several still-open questions that for now inhibit our ability to provide a comprehensive and quantitative modeling framework for RIS.

## II. QUANTIFYING SOLUTE/PD FLUX COUPLING WITH TRANSPORT COEFFICIENTS

As explained above, the flux coupling between the atoms belonging to the alloy and the PDs produced by irradiation is quantified by the off-diagonal transport coefficients of the Onsager matrix. These coefficients are, therefore, the foundation stone of any attempt to model the RIS phenomenon at a scale where atoms are not explicitly considered, and such modeling scale is desirable given the intrinsic multi-scale nature of RIS. Unfortunately, it is generally not possible to obtain the full Onsager matrix of a system using experimental measurements only,<sup>14</sup> which is why these coefficients have to be computed. In this section, we shall review the state-of-the-art of flux coupling coefficient calculations as well as current efforts directed toward overcoming the usual limitations of such studies.

### A. From atomic trajectories to transport coefficients

Diffusion of PDs and atoms proceeds via successive jumps from one lattice site to a neighboring one, these jumps being performed by overcoming a migration barrier. Depending on the local configuration of the system, several migration barriers can be available and the transport coefficients convey the average kinetic behavior of the system.

Knowing that, it seems natural to try to simulate the full dynamics of the atoms and measure the relevant quantities to obtain the transport coefficients, i.e., the mean square displacements measured along a trajectory,<sup>17</sup>

$$L_{\beta\alpha} = \frac{\langle \mathbf{R}(\beta) \cdot \mathbf{R}(\alpha) \rangle}{6\tau V}, \quad (4)$$

where the brackets denote a thermodynamic average and  $\mathbf{R}(\alpha)$  represents the total displacement vector for all atoms of species  $\alpha$

during time  $\tau$  in a system of total volume  $V$  placed at temperature  $T$ . Molecular dynamics methods simulate such a dynamics, but it requires a precise interatomic potential, and existing potentials are rarely developed with a focus on the migration properties of PDs, especially in concentrated alloys. Moreover, computational limitations confine the dynamics to short time-scales only and the PD while solute jumps are infrequent events. Therefore, it is usually complicated to obtain converged values of transport coefficients, and despite the existence of alternative methods to increase the time scale<sup>18–20</sup> and estimate the expected error on the measured coefficients,<sup>21</sup> molecular dynamics is still far from being routinely used to compute flux coupling coefficients. One exception is the study of SIA migration because they have very low migration barriers in various systems, and therefore, the migration events are not so infrequent.<sup>22,23</sup>

The use of on-lattice atomic kinetic Monte Carlo (AKMC) simulations for this purpose is much more standard. In AKMC simulations, the vibrations of the atoms are not modeled explicitly and each step of the method consists in realizing a solute or PD jump on a rigid lattice with effective interactions between atoms and PDs. It is assumed that successive jumps form a Markov chain, which allows the use of various statistical physics tools. AKMC simulations are routinely used to measure diffusion coefficients and sometimes also for flux coupling coefficients,<sup>24</sup> but for the latter, the numerical measure can be very hard to converge for some systems, especially dilute ones or systems with a weak coupling. Also, kinetic trapping is a common issue in AKMC simulations, which triggered the development of various sophisticated algorithms,<sup>25–28</sup> even though they have not been yet applied to the study of RIS.

One of the advantages of molecular dynamics is that it is an off-lattice method that does not presuppose any migration mechanism.<sup>29</sup> The off-lattice AKMC counterpart also exists, at the cost of increased computational cost<sup>30–32</sup> compared with standard AKMC. Up to now, such approaches have not been applied to the study of RIS.

These numerical methods are easily implemented, but their stochastic nature induces statistical errors in the results which are not always admissible (especially, for flux coupling coefficients in dilute systems). Moreover, a whole new simulation must be carried out each time a parameter changes (solute or defect concentration, temperature, and strain), rendering this approach unpractical for systematic studies.

For this reason, a lot of effort has been put into developing deterministic methods. One of them is the Onsager code<sup>33</sup> which uses Green's function approach to integrate kinetic trajectories of infinite range but is limited to vacancy-mediated solute diffusion in the very dilute limit (i.e., a single substitutional solute interacts with a single vacancy). Another one is the KineCluE code,<sup>34</sup> which is an implementation of the self-consistent mean-field method.<sup>35</sup> In KineCluE, kinetic trajectories are truncated at some convergence point, but the code is able to treat almost any defect or small atom-defect cluster (up to 5 or 6 components depending on the system) and their migration mechanisms, including collective mechanisms involving several atoms/defects. Both codes are open-source. They apply to dilute systems only and they require the same kind of inputs: the energy of the various configurations and migration barriers available in the system.

## B. *Ab initio* calculation of configuration energies and migration barriers

The most accurate methods available to us to evaluate an energy landscape are the so-called *ab initio* methods and their implementation within the density-functional theory (DFT) formalism. Of course there are some alternatives offering a higher computational efficiency at the cost of lower accuracy: tight-binding models, semi-empirical potentials, cluster expansions, and nowadays machine learning potentials, but at some point, these alternatives require fitting to some *ab initio* set of data. Therefore, we focus this paragraph on DFT calculations only.

The DFT calculation of a large set of configuration and migration energies is computationally expensive, but it is accessible to modern supercomputers. High-throughput DFT studies have been dedicated to the calculation of flux coupling coefficients for a series of solutes in various cases: vacancy and substitutional solute coupling in Mg,<sup>36</sup> Zr,<sup>37</sup> Fe,<sup>38,39</sup> and various cubic metals<sup>40,41</sup> as well as substitutional solute coupling with both vacancies and SIA in Fe<sup>42</sup> and Ni,<sup>43</sup> the latter providing a rigorous derivation of the kinetic properties even though the results are mostly in line with previous studies involving more approximations.<sup>44,45</sup> Nevertheless, note that results for Ni must be taken with care as paramagnetism was not accounted for while the Curie point of Ni is fairly low. All these calculations were assuming dilute alloys to make use of the deterministic methods mentioned above and to reduce the extent of phase space, i.e., the number of configuration and migration barriers to compute.

Similar high-throughput DFT studies are now feasible also for larger clusters involving several PDs and/or solutes.<sup>46</sup> Up to now, such studies have been restricted to configuration energies, but surely migration energies will follow in a near future, even more so knowing that there are deterministic methods<sup>34</sup> available to transform these data into valuable transport coefficients. An example of such calculation of transport coefficients for a less dilute system (i.e., involving PD-solute clusters larger than pairs) exists.<sup>47</sup>

The next step forward is to go to concentrated alloys, where an exhaustive calculation of all possible local configuration and migration energies becomes unfeasible, even when resorting to simplified models that are computationally more efficient than DFT calculations. The gigantic phase space associated with concentrated alloys must, therefore, be sampled, and AKMC methods are up to now the reference methodology to measure flux coupling coefficients in such systems<sup>24</sup> or simply diffusion coefficients.<sup>48</sup> Concentrated alloys draw a lot of attention because some of these alloys are actually used in nuclear power plants, but also because of the growing interest for the so-called high entropy alloys or multi-principal element single-phase solid solutions that are credited with a particular resistance to RIS and irradiation effects in general.<sup>49–51</sup> Large databases of DFT calculations of configuration and migration energies are appearing for these systems,<sup>48,52,53</sup> but the rigorous statistical thermodynamics model is now needed to guide the elaboration of such databases and make the most of the obtained data. In this direction, there is some work aiming at inferring meaningful properties directly from the distributions of energies,<sup>54</sup> but this work is not sufficiently mature yet to be applied to RIS.

It is known that RIS depends on the sink PDs diffuse to. For instance, the grain boundary (GB) character and orientation will

result in different RIS values.<sup>55–57</sup> This is mainly due to the strain field developed around the sink that modifies the energetic landscape of both PDs and solutes and, therefore, the flux coupling coefficients. The elastic dipole formalism<sup>58–61</sup> is the easiest way to account for configuration and migration energy changes around the sink, mostly because the elastic dipoles themselves are easily obtained from standard DFT calculations. It has been used extensively to study the absorption of PDs by sinks and RIS, combined with various simulation techniques for the calculation of transport coefficients<sup>62–70</sup> but to date most of these calculations are performed in pure systems. Note that for concentrated alloys, large energy and elastic dipole databases are starting to appear.<sup>71</sup>

The energetic landscape can change quite dramatically with temperature, yet standard DFT calculations are performed at 0 K. Fortunately, there are some methods to compute—or at least approximate—temperature effects in DFT calculations.<sup>72</sup> In the diffusion community, people have been quite routinely computing the vibrational entropy contribution that directly relates to the attempt frequency of a jump in the harmonic approximation of transition state theory.<sup>73</sup> These calculations remain cumbersome, and their convergence with respect to box size is far from obvious.<sup>74</sup> Machine learning techniques could offer an efficient response to this matter.<sup>75</sup> Yet, the analysis of several sets of data shows that attempt frequencies do not vary much (usually within a factor of 2 or 3) for a given cluster of PDs and solutes, and the overall effect on transport properties is usually fairly low, especially knowing the computational effort required to quantify it.<sup>39,40</sup>

A more rigorous treatment of temperature effects requires to go beyond the harmonic approximation and to integrate anharmonic effects as well. This kind of calculation started for configuration energies,<sup>76</sup> and it is nowadays being generalized to migration energies, with unsupervised routines.<sup>77,78</sup>

Another aspect of energetic calculations that is not necessarily easy to account for properly is magnetism. This point is important because the structural materials of nuclear reactors are mostly steels showing very specific magnetic properties. Recent works have been studying the interplay between magnetic and chemical degrees of freedom in concentrated alloys,<sup>71</sup> as well as the impact of magnetic ordering and relaxation on vacancy diffusion combining DFT data and AKMC simulations.<sup>79,80</sup> A study of the impact of magnetic ordering on RIS should be technically feasible in the coming years, even though the correct modeling of paramagnetic system remains a challenge.

As an example, we will now present in more details state-of-the-art calculations of flux coupling coefficients and RIS factors from DFT data.

## C. Examples of flux coupling and RIS calculations from atomic-scale data

In Ref. 42, the authors present a comprehensive study of RIS in dilute alloys for a variety of solutes in  $\alpha$ -Fe, considered as perfectly ferro-magnetic. Using standard DFT calculations at 0 K, the energy of PD-solute interactions was computed up to the fifth nearest-neighbor for both vacancies and SIAs. All the symmetry unique migration energies within this range were also computed as well as attempt frequencies in harmonic approximation. Then, the

transport coefficients for isolated PDs and PD-solute pairs were obtained using the KineCluE code.<sup>34</sup> The proportion of isolated PDs vs PDs paired with a solute is obtained assuming local equilibrium with respect to the nominal concentration of PDs. The transport coefficients are then inserted in the Wiedersich theory, which is the standard analytical model for RIS based on atomic and PD flux equations at steady state.<sup>81,82</sup> Wiedersich's theory is simply deduced from a stationary condition applied to Eq. (3) and its equivalent for solutes. Note that RIS stems from the dynamic creation and removal of PDs, which maintains the segregated atoms out-of-equilibrium. Therefore, the atom chemical potentials are not homogeneous in the system (especially, near PD sinks where RIS occurs), which, according to Eq. (1), gives rise to atomic fluxes directed against the RIS profile. This contribution to RIS is known as backward diffusion.

In the following, from the  $L_{\alpha\beta}$  adapted version of Wiedersich's formulae<sup>14,82</sup> (the original version being written in terms of partial diffusion coefficients), we define the steady-state RIS factor as  $\alpha/X_B = -\nabla \ln X_B / \nabla \ln X_V$ , with  $\alpha$  equal to

$$\alpha = \frac{L_{AI}L_{AV}}{L_{AI}D_B + L_{BI}D_A} \left( \frac{L_{BV}}{L_{AV}} - \frac{L_{BI}}{L_{AI}} \right), \quad (5)$$

where A, B, V, and I represent the matrix atom, solutes, vacancies, and SIAs, respectively;  $X_B$  ( $X_V, X_I$ ) is the solute (vacancy, SIA) fraction, and  $D_A$  ( $D_B$ ) is the intrinsic diffusion coefficient of matrix (solute) atoms. A positive (negative) RIS factor leads to solute enrichment (depletion), and Eq. (5) shows that the off-diagonal transport coefficients are indeed key quantities for the modeling of RIS. The RIS behavior of each solute as a function of temperature is reported in Fig. 1, and we highlight that it stems from a

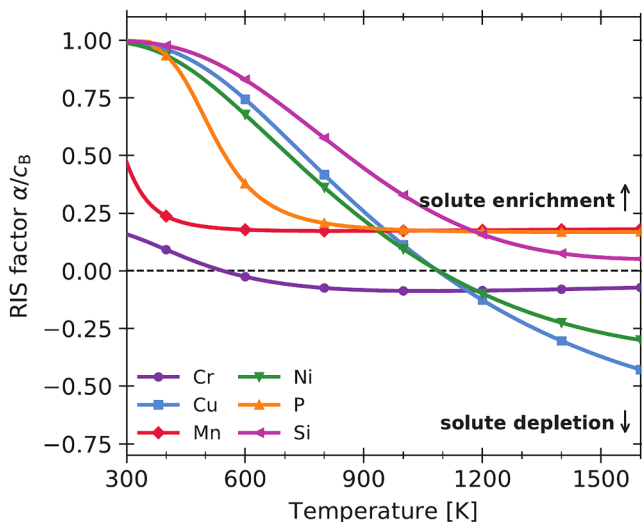


**FIG. 1.** RIS factor for various solutes in  $\alpha$ -Fe, which provide the RIS tendency at PD sinks (solute enrichment or depletion).<sup>42</sup>  $c_B$  is the solute concentration ( $X_B$  in our notations). Reproduced with permission from Messina *et al.*, *Acta Mater.* **191**, 166 (2020). Copyright 2020 Elsevier.

competition between SIA-solute flux coupling and vacancy-solute flux coupling.

The previous study is limited to small solute concentrations (typically lower than 1 at. %) because it was assumed that a single solute interacts with a single PD. The next natural step is, therefore, to include the interaction of several solutes with several PDs in the calculation of transport coefficients. This is the aim of the kinetic cluster expansion method developed in conjunction with the KineCluE code<sup>34</sup> and illustrated in Ref. 47. This paper focuses on ferromagnetic  $\alpha$ -Fe that contains interstitial solutes C and O as well as vacancies. The configuration and migration energies of the system are computed from a cluster expansion model fitted to *ab initio* data of small vacancy-interstitial solute clusters.<sup>83</sup> The modeling of the energetic landscape is, thus far, less accurate than in the previous publication, but the drag ratio of C by vacancies, for instance, has a more sophisticated expression,

$$\frac{L_{CV}}{L_{VV}} = \frac{\sum_{\gamma} X_{\gamma} L_{CV}(\gamma)}{\sum_{\gamma} X_{\gamma} L_{VV}(\gamma)}, \quad (6)$$

where  $\gamma$  represents a vacancy-solute cluster,  $X_{\gamma}$  is the fraction (per lattice site) of cluster  $\gamma$ , and  $L_{CV}(\gamma)$  is the off-diagonal transport coefficient associated with a single  $\gamma$  cluster. The clusters involved in the numerator are clusters containing both vacancies and C atoms ( $VC, VC_2, V_2C, V_3C$ , and  $VOC$ ) while the clusters involved in the denominator are all clusters containing vacancies ( $V, V_2, V_3, VB, VB_2, V_2B, V_Bx, VOC, B = C, O$ ). The computed drag ratio is reported in Fig. 2.

This figure shows that the magnitude—and more importantly the sign—of the flux coupling coefficient varies according to the local concentration of both species, and this is caused by the fact that a different cluster dominates the kinetic properties in each concentration range. If the  $VC$  cluster was the only one considered, then the flux coupling coefficient would be negative over the whole plot.

On a side note, bear in mind that there have been some questions raised about PD production and interaction with displacement cascades. Following previous models of ballistic mixing,<sup>84,85</sup> recent works<sup>86</sup> have shown that the continuous formation of displacement cascades in the course of irradiation might affect transport coefficients and therefore RIS factors when the effective ballistic jump frequencies are of the order of magnitude of relevant thermal jump frequencies. Also, it is generally assumed that displacement cascades produce isolated PDs or PD clusters, but it has been shown that PD-solute binding also plays a role<sup>87</sup> and can significantly alter the relative quantities of mixed SIAs vs pure SIAs compared with the usual assumption that the relative probability of these two types of PD state follows a local equilibrium assumption with respect to the local solute and PD concentrations. Flux coupling coefficients being mostly computed under such an assumption, the resulting RIS profile might get affected by the solute-PD population created by the displacement cascade, especially for microstructures with a high density of PD sinks since PDs would eliminate before recovering the local equilibrium distribution of PD-solute clusters. This topic definitely requires further investigation.

The calculations presented in this section do not treat explicitly the sinks and their ability to absorb supersaturation of PDs.

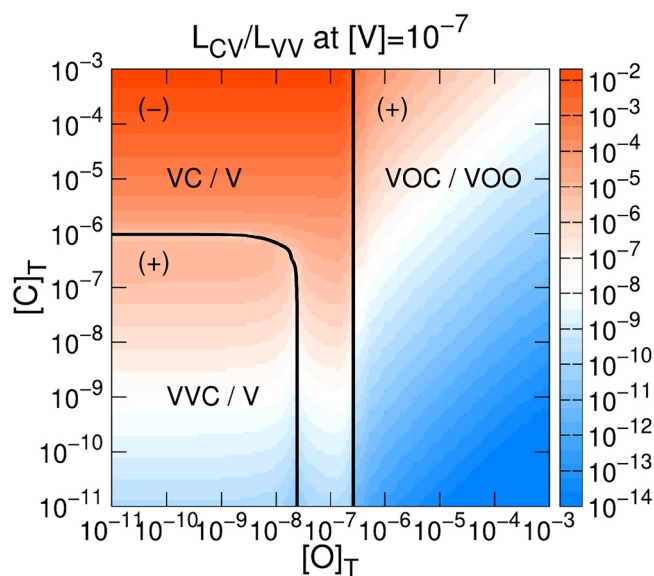


**FIG. 2.** Drag ratio of carbon atoms by vacancies at constant vacancy concentration (10 appm) and temperature (500 K) as a function of C and O concentration.<sup>47</sup> In each region, the sign of the drag ratio is indicated as well as two cluster names: the dominating cluster in the numerator/denominator of Eq. (6).  $[B]_T$  represents the nominal fraction of atoms of species  $B$ . Reproduced with permission from Schuler *et al.*, *Phys. Rev. Mater.* **4**, 020401(R) (2020). Copyright 2020 American Physical Society.

Besides, it is implicitly assumed that kinetic properties are homogeneous throughout the system, which may be unrealistic since strain fields develop around PD sinks, and these strain fields modify transport coefficients and therefore RIS. To go further, an explicit model of the PD sink is required.

### III. MODELING OF RIS WITH STATIC PD SINKS

As explained in the Introduction, the annihilation of PDs at sinks necessarily causes a reorganization of the sink structure: dislocations will climb, cavities and dislocation loops will grow or shrink by absorbing PDs. As a first step, most studies assume that the solute concentration profile evolves much faster than the sink structure and therefore consider RIS on immobile or static sinks. We will quickly present the different simulation methods used for this, before focusing on the results on body-centered cubic (bcc) Fe–Cr alloys that have received most attention recently as a model for ferritic steels. Some simulations in austenitic alloys and other systems of industrial interest will be also briefly discussed.

#### A. Simulation methods

In principle, once the thermodynamic properties and transport coefficients of a system are known, the reaction-diffusion equations [Eqs. (1) and (3)] can be solved numerically (either in terms of diffusion coefficients and concentration gradients or in terms of Onsager coefficients and chemical potential gradients) to

follow the evolution of the solute concentration profiles around a given PD sink such as a dislocation or a GB, for instance. This has been the standard procedure since the first models of RIS (see Ref. 14, and references within), but it has been greatly improved recently with the development of methods enabling a better estimation of the transport coefficients from accurate DFT calculations of atomic jump frequencies, as explained in Sec. II.

If one assumes that the elimination of PDs by recombination is negligible everywhere,<sup>82</sup> or at least in the vicinity of the sinks,<sup>9</sup> one can derive analytical expressions of solute and PD segregation profiles or the total amount of solute  $B$  segregated at a sink,  $S_B$ . This approach has been used by Huang *et al.* in the case of 1D RIS profile at GBs to build systematic maps of  $S_B$  as a function of temperature  $T$ , dose rate  $G$ , and total sink strength  $k^2$  in bcc Fe–B dilute alloys.<sup>9</sup> An example is shown in Fig. 3, with the total amount of segregated solute atoms  $S_B$  in various Fe–B alloys, as a function of the dose rate and temperature for a given sink strength (note the atypical behavior of the Fe–Cr system, with an inversion of the segregation between low and high temperatures). The same authors also take into account other factors, such as the ballistic mixing that tends to reduce flux coupling and homogenize the solute concentration and, therefore, to limit RIS (the effect is stronger in the immediate vicinity of the sinks, because PD concentrations are lower there and ballistic mixing, therefore, becomes the dominant diffusion mechanism). The effect of elastic interactions on the driving forces<sup>88,89</sup> and on the migration barriers<sup>88,90</sup> has also been considered.

The application of AKMC simulations to the modeling of irradiation effects has been recently reviewed.<sup>91</sup> Early AKMC simulations were dealing with model systems,<sup>92–96</sup> but the modeling of specific alloys based on DFT calculations recently became possible.<sup>24,82,97</sup> AKMC simulations benefit from the fact that spatial and temporal correlations are fully taken into account. This is, of course, especially important for kinetic correlation effects that affect transport coefficients and solute/PD flux coupling, but also for the recombination between vacancies and SIAs<sup>98</sup> and the local fluctuations of composition. Therefore, transport coefficients do not need to be computed beforehand when using AKMC methods, the key point being a good description of migration barriers. Another important advantage of AKMC simulations is that they can simulate the nucleation of precipitates, which can result from RIS (a phenomenon known as Radiation Induced Precipitation, or RIP) or interfere with it.<sup>99</sup>

Finally, Phase Field (PF) and reaction-diffusion models have been used to model different irradiation effects,<sup>100–102</sup> including, more recently, RIS.<sup>95,102–105</sup> They can include the full Onsager matrix (which must, however, be provided by another method, cf. Sec. II) to deal with solute/PDs coupling and elastic effects. They are more suitable than AKMC simulations for modeling elastic effects and off-lattice features such as dislocation loops, since they solve a set of continuous partial differential equations at the mesoscopic scale. In principle, they should also allow for larger time and space scales—although this is not obvious from the existing studies of RIS, which are often limited to 1D or 2D descriptions. Dealing with the nucleation of precipitates with PF methods remains challenging.<sup>106–108</sup> It was shown<sup>106</sup> that to obtain the correct thermal fluctuations of composition in an alloy arbitrarily divided

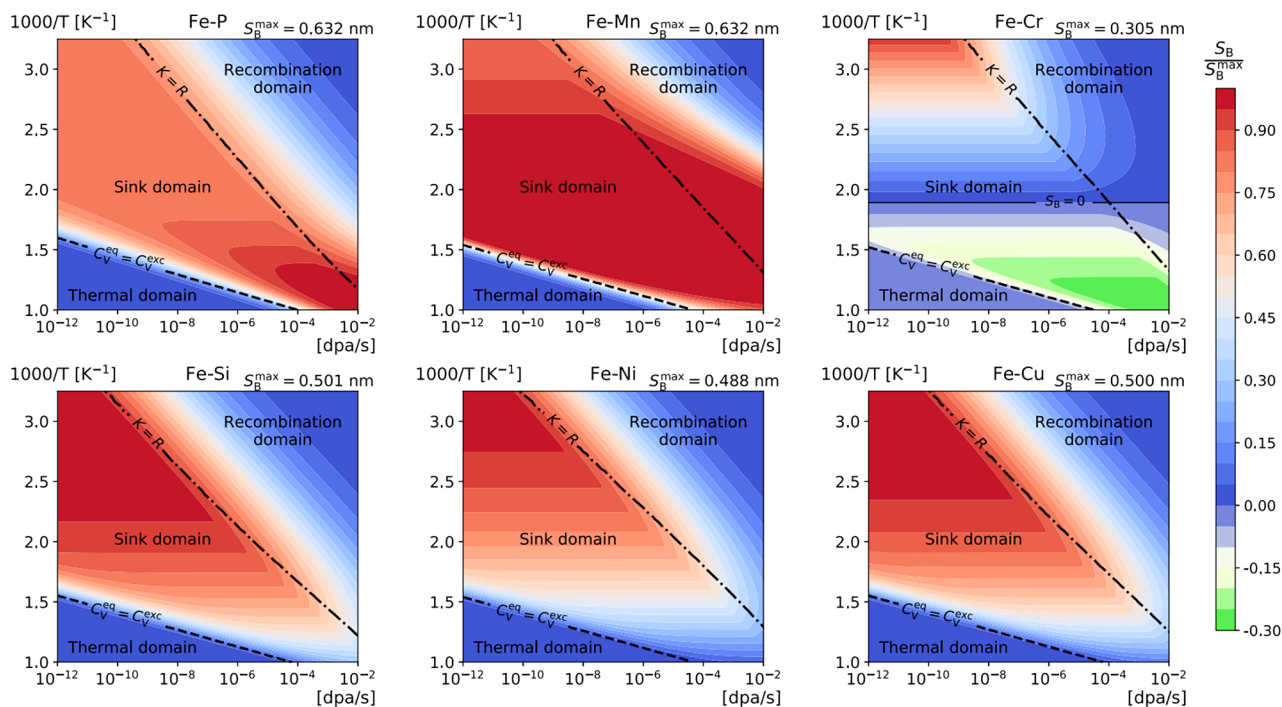


**FIG. 3.** Total amount of segregated solute atoms  $S_B$  as a function of dose rate (in dpa/s) and inverse temperature (in  $K^{-1}$ ) for several dilute binary Fe – B alloys, computed by Huang *et al.*<sup>9</sup>  $S_B$  is normalized by its maximum,  $S_B^{\max}$ , over all considered irradiation conditions. The nominal solute fraction,  $X_B$ , is set to 1 at.% and the sink strength  $k^2 = 5 \times 10^{14} \text{ m}^{-2}$ . Reproduced with permission from Huang *et al.*, Phys. Rev. Mater. **5**, 033605 (2021). Copyright 2021 American Physical Society.

into cells, cell-size-dependent models of the Cahn–Hilliard energy density and gradient energy are required. These cell-size-dependent energies can be extracted from equilibrium AKMC simulations.<sup>106,107</sup> However, a coarse-grained method relies on a local equilibrium assumption within the dividing cells. Unless the critical nucleus is greater than the dividing cell, the nucleation stage becomes an instantaneous event. Therefore, we expect such PF modeling methods of precipitation to be quantitative only as long as the critical nucleus is significantly greater than the dividing cell, as observed in Ref. 106. On the other hand, phase transformations in unstable solid solutions in the spinodal decomposition regime are correctly treated by PF models as long as the interfacial energy is set to a physically meaningful value. An alternative method is to introduce critical clusters with a nucleation rate computed from the classical nucleation theory.<sup>108,109</sup> The latter accurately describes nucleation in weakly supersaturated binary alloys, but its extension to multi-component or more highly supersaturated alloys is difficult.

Regarding the coupling between elasticity and diffusion, a whole variety of studies have been devoted to the computation of sink strength: analytical models,<sup>110</sup> AKMC,<sup>62</sup> Object Kinetic Monte Carlo (OKMC),<sup>63–65</sup> PF,<sup>66–69</sup> or mixed PF/AKMC<sup>70</sup> approach. The comparison between these studies emphasizes interesting differences depending on the modeling methods and especially the boundary conditions.<sup>89</sup>

## B. RIS in Fe–Cr alloys

All these techniques have been recently applied to study RIS in bcc Fe–Cr alloys as a model of ferritic steels. Wharry and Was<sup>111</sup> solved the reaction-diffusion equation [Eq. (3)] to model Cr segregation at GBs with Perk’s model, which assumes that the partial diffusion coefficients of Fe and Cr by vacancy and SIA mechanisms are controlled by a single migration barrier. Within this model, they found that the behavior of dilute Fe–Cr alloys is controlled by inverse Kirkendall effects: Cr diffuses faster than Fe, via both the vacancy and SIA migration mechanisms. The negative Cr–vacancies coupling favors a Cr depletion at sinks, and the positive Cr–SIA coupling favors a Cr enrichment. The latter prevails at low and moderate temperatures. The model also predicts that an increase in Cr concentration (from 9 to 15 at.%) results in a decrease in Cr enrichment at GBs. The competition between the vacancy and SIA is confirmed by detailed studies of transport coefficients using DFT calculations of PD migration barriers and the KineCluE code<sup>38,42</sup> (in the dilute limit) and by AKMC simulations<sup>24</sup> (for Cr concentrations up to 15 at.%). The behavior of Cr in Fe is indeed quite different from that of many other solutes, insofar as the Cr–vacancy interaction is very weak and almost no vacancy drag effect is expected in the range of temperature where RIS occurs. These conclusions are consistent with some experimental observations in the Fe–Cr model and industrial alloys with 9–12 at.%Cr,<sup>111</sup> but not with all of them. RIS experiments in ferritic alloys are indeed

particularly difficult to interpret, revealing no obvious link between the Cr depletion or enrichment at GBs and the composition of alloys or irradiation conditions.<sup>112</sup> The simulations explain the origin of these difficulties: the balance between the vacancy and SIA contributions to RIS is very delicate, i.e.,  $L_{CrV}/L_{FeV}$  and  $L_{CrI}/L_{FeV}$  terms in Eq. (5) have both significant but similar values, and small variations in the local Cr concentration (or the effect of other alloying elements), elastic effects, ballistic mixing, magnetic transition, etc., can, therefore, tip the RIS in one direction or the other.

The AKMC simulations of Senninger *et al.*<sup>24</sup> give the same general trends as diffusion equations of Wharry and Was:<sup>111</sup> a positive coupling between SIA and Cr, a negative coupling between vacancies and Cr, a Cr enrichment at sinks at low temperatures, a depletion at higher temperatures. For 10 at.%Cr, the inversion occurs at 800 K, which is close to the results obtained for 9 at.%Cr with diffusion equations. AKMC simulations also predict that an increase in Cr concentration between 5 and 15 at.% reduces the enrichment tendency (but it is enhanced between 0 and 5 at.%Cr). In the dilute limit, the inversion between enrichment and depletion occurs at 550 K, which is close to the value obtained from the DFT calculation of the migration barriers and the KineClue code combined with Eq. (5) (see Fig. 1 and Ref. 42). It seems however that the AKMC simulations overestimate the negative flux coupling between Cr and vacancies (see Fig. 5 in Ref. 38).  $L_{CrV}$  is always positive, while the results of Messina *et al.* predict that it becomes negative at low temperatures (below 300 K).<sup>42</sup> More generally, it should be also noted that such AKMC simulations are expected to give a good description of diffusion properties of the underlying PD jump frequency model. The one used in Ref. 24 is based on effective pair interactions and the parameters controlling its diffusion properties are fitted to DFT calculations of vacancy and SIA migration barriers in dilute Fe and Cr alloys. Such simulations could be improved by using a larger DFT database, including concentrated alloys.

The same AKMC simulations have been used to study the effects of grain size on RIS<sup>82</sup> (see Sec. IV below). At low temperatures, it is found that the enrichment of Cr at GBs is sufficient to produce RIP in under-saturated Fe–Cr solid solutions<sup>24,82</sup> (e.g., in Fe-9 at.%Cr at 563 K). The microstructure of Cr precipitation at GBs can be rather complex due to the equilibrium segregation that can strengthen or oppose the RIS<sup>113</sup> and to depletion in PD concentrations near the sinks, which results in a decrease in Cr diffusion and in precipitate-free zones near the GBs.<sup>24,82,113</sup> AKMC simulations show that the microstructure of precipitation of the Cr-rich  $\alpha'$  phase in supersaturated alloys (which may be considerably accelerated by irradiation) is also affected by the same mechanisms (precipitate-free zones have been observed experimentally near GBs and incoherent precipitate/matrix interfaces in Fe-15 at.%Cr alloys under neutron irradiations<sup>114</sup>).

A PF model has been applied to the study of RIS in Fe–Cr by Piochaud *et al.*<sup>103</sup> A standard PF model for Fe–Cr alloys (a system with a conserved order parameter) would be based on a Cahn–Hilliard equation and would include the free energy of homogeneous Fe–Cr alloys without PDs, a stiffness parameter  $\kappa$  controlling the energetic cost of concentration heterogeneities and a scalar mobility coefficient  $M$  controlling the diffusion properties.

To deal with RIS, such standard PF model must be modified on several points:

- since PDs are not at equilibrium, the PD driving forces depending on the gradients of vacancies and SIA chemical potentials must be taken into account, in addition to the gradient of the solute [or the difference  $\mu_{Cr} - \mu_{Fe}$ , cf. Eq. (1)];
- the mobility coefficient  $M$  must be replaced by the full matrix of Onsager coefficients;
- effective stiffness parameters  $\kappa_V$  and  $\kappa_I$  must be introduced. Unlike  $\kappa$ , they do not reduce to a thermodynamic contribution but include a kinetic part that depends on diffusion mechanisms and correlation effects.<sup>115</sup> The effect on the RIS—which only involves smooth concentration profiles—is small, but it is believed that it would be significant in the case of  $\alpha'$  precipitation. Note that in most other PF studies applied to RIS, even the standard interfacial energy term, the stiffness coefficient  $\kappa$ , is ignored. Such an approximation reduces the PF equations to standard reaction-diffusion equations [Eq. (3)].

All PF parameters have been fitted to the thermodynamic and diffusion model of Senninger *et al.*<sup>24</sup> Overall, one gets a good agreement with AKMC simulations for the kinetics and steady-state concentration profiles (Fig. 4): the Cr enrichment and depletion trends at GBs are the same as in Ref. 24. Thanks to their relatively lower computational cost, systematic 2D-PF simulations can be performed more easily than with AKMC simulations to study the effect of temperature, composition, etc., and in larger systems. The effect of simplifying assumptions used in other models [which can neglect the dependence of transport coefficients on local composition or use an ideal solution model with a thermodynamic factor set to (1)] can be assessed and are found to be often significant.<sup>103</sup> Finally, the PF model was modified to take into account the thermally activated formation of PD at sinks, which was ignored in AKMC simulations: in the absence of irradiation, the model, therefore, drives the systems toward its equilibrium PD concentrations, and under irradiation, this results in a lower (and finally in a vanishing) RIS when the temperature increases.

One of the key advantages of PF models is probably their ability to deal with strain effects, long-range elastic interactions, and off-lattice defects such as dislocations.<sup>104,105</sup> The elastic interactions between sinks, solute atoms, and PDs had been neglected in the previous studies of RIS at GBs, which can be partly justified by the fact that GBs are usually neutral sinks, with the same sink strength for vacancies and SIAs and absorbing both at the same rate in the steady-state. The situation is not the same in the case of RIS at dislocations that are biased sinks interacting more strongly with SIAs (as long as RIS does not change this tendency). Thuinet *et al.*<sup>104</sup> modified the PF model of Ref. 103 to study RIS on dislocation dipoles in Fe–Cr alloys: all the thermodynamic and kinetic parameters are the same, but eigenstrain parameters are introduced for the interactions between the dislocations and vacancies and between the dislocations and SIAs (the interaction between the dislocations and Cr atoms is neglected because of the small lattice mismatch between Fe and Cr).

Without these elastic interactions, the RIS tendencies at dislocations are the same as at GBs (being controlled by same transport

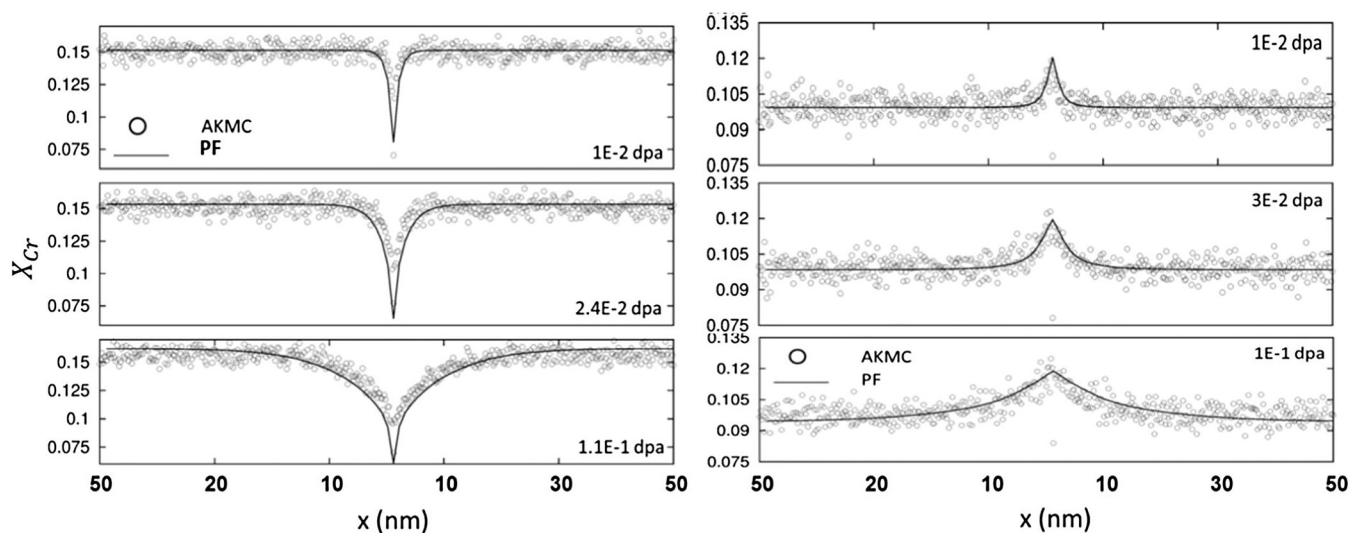


**FIG. 4.** RIS profiles obtained using AKMC (symbols) and PF (lines) in Fe-15 at. %Cr at 900 K (left) and in Fe-10 at. %Cr at 700 K (right), as a function of the distance from the GB,  $x$ , and for different irradiation doses at a dose rate of  $10^{-5}$  dpa  $s^{-1}$ .<sup>103</sup> Reproduced with permission from Piochaud *et al.*, *Comput. Mater. Sci.* **122**, 249 (2016). Copyright 2016 Elsevier.

coefficients). But elastic interactions can significantly modify this behavior. An example is shown in Fig. 5 for Fe-15 at. %Cr alloys irradiated at  $T = 900$  K, with a dose rate  $G = 10^{-5}$  dpa  $s^{-1}$ . Without elasticity, one observes a depletion of Cr around dislocation cores [Figs. 5(b) and 5(c)] as on GBs [Fig. 4(a)]. With elastic interactions [Figs. 5(d) and 5(e)], one observes a local inversion, with a Cr enrichment in the traction zones that can be explained by the fact that vacancies are more attracted by the compression zones and the SIAs by the traction zones. The same PF model has been recently modified to include the climb of isolated dislocations loops or dislocations within symmetric tilt GBs and its effects on RIS,<sup>105</sup> as will be explained in Sec. IV.

Finally, the OKMC method has been used by Balbuena *et al.*<sup>116</sup> to model precipitation and segregation in Fe-Cr alloys under irradiation. Including thermodynamic properties very similar to the previous AKMC and PF models, it can be considered as an intermediary method between them, seeking to combine their advantages. It can also reproduce the same Cr/PDs flux couplings and, therefore, could be used in the future for simulations of RIS. However, in this kind of cellular Monte Carlo methods, the same finite-size and local equilibrium issues already discussed for PF methods also apply.

### C. RIS in Fe-Ni-Cr alloys and other systems

RIS has been first observed in austenitic steels based on the face-centered cubic (fcc) Fe-Ni-Cr system, and the situation is experimentally much clearer than in ferritic steels, at least for major elements: one usually observes a depletion of Cr and an enrichment in Ni at PD sinks. It has long been observed that the tracer diffusion coefficients measured during isothermal annealing (i.e., with only a vacancy diffusion mechanism) in these alloys follow the order  $D_{Cr}^* > D_{Fe}^* > D_{Ni}^*$ .<sup>117</sup> Therefore, observed

tendencies correspond to what could be expected when RIS is controlled by the negative coupling between atoms and vacancies and the inverse Kirkendall effect. For this reason, the contribution of SIAs is often believed to be negligible or to reinforce the one of vacancies, contrary to what happens in the bcc Fe-Cr alloys. Many diffusion models, based on such assumptions, qualitatively reproduce the experimental trends (for a recent review, see Ref. 14).

On the other hand, the atomistic modeling on fcc Fe-Ni-Cr alloys is less advanced than the ones on bcc Fe-Cr alloys. One of the reasons is probably that the fcc Fe-Ni-Cr system is more complex because it is a ternary system but also because austenitic alloys are paramagnetic. The magnetic disorder should, in principle, be taken into account in diffusion models (and in DFT calculations used to parameterize them). Bcc alloys based on Fe-Cr systems are usually ferromagnetic if the temperature and the Cr concentrations are not too high. To our knowledge, at the present time, no model integrates the complete Onsager matrix, with transport coefficients deduced from an atomic model of jump frequencies in concentrated fcc Fe-Ni-Cr alloys. A first attempt using AKMC simulations has been made by Piochaud *et al.*<sup>118</sup> using a constant pair interaction model, fitted to DFT calculations of PD properties on stable positions. They do not reproduce some experimental RIS tendencies, since they predict a depletion of Ni at GBs. The authors conclude that the diffusion model should be improved to include saddle-point configurations in the fitting of the model to DFT calculations, and that the magnetic disorder should be accounted for as well. One of the most recent models for Fe-Ni-Cr alloys, developed by Rezwan *et al.*<sup>119</sup> to deal with RIS during grain growth (see Sec. IV), is still based on the MIK model using a single effective vacancy migration energy for each species and assuming that RIS is controlled by the inverse Kirkendall effect, while SIA diffusion is assumed to have a negligible impact on RIS.

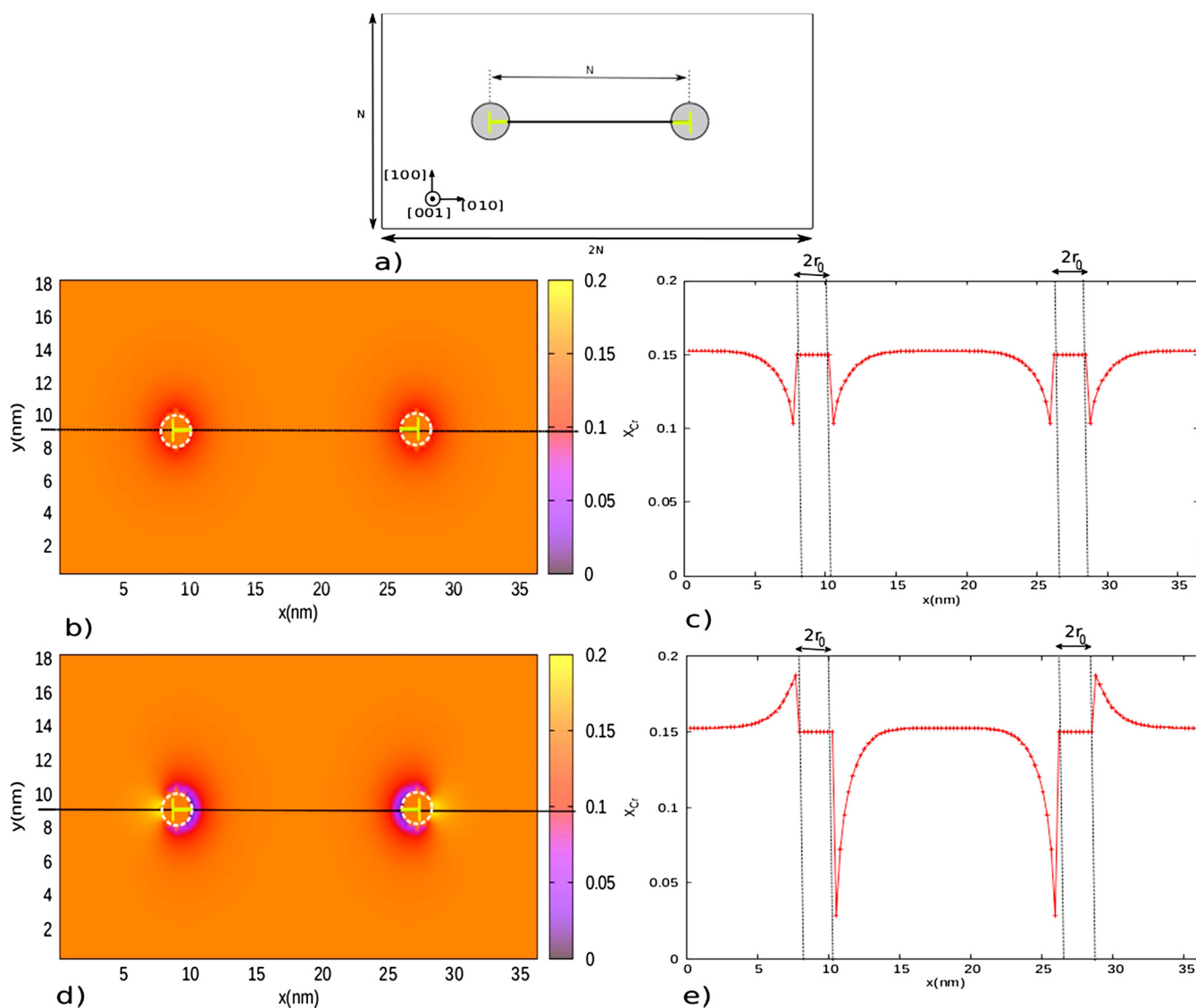


**FIG. 5.** (a) Representation of the dislocation dipole considered for PF simulations of RIS.<sup>104</sup> Cr composition map for Fe-15 at. %Cr at 900 K and  $10^{-5}$  dpa  $s^{-1}$  (b) without elasticity and (d) with elasticity. Corresponding Cr profiles along the direction indicated in the dashed line on the maps (c) without elasticity and (e) with elasticity. Vertical dashed lines on (c) and (e) indicate the positions of the absorbing cores. Reproduced with permission from Thuinet *et al.*, *Comput. Mater. Sci.* **149**, 324 (2018). Copyright 2018 Elsevier.

Therefore, the fact that it is easier than in ferritic steels to identify major trends in the enrichment or depletion of a particular solute does not mean that quantitative predictive models are available. Even in simpler Ni-based binary alloys, the situation is not completely clear. For example, experimental observations of Allen *et al.*<sup>120</sup> in Ni-18 at. %Cr alloys show (except in one case) a depletion of Cr at GBs. On the contrary, the segregation profiles calculated by Barnard *et al.*<sup>121</sup> with a diffusion model based on DFT calculations of Tucker *et al.*<sup>44</sup> show an enrichment of Cr (dominated by a positive coupling between Cr and self-interstitials).

Calculations of transport coefficients with the KineCluE code based on DFT calculations<sup>43</sup> also predict a Cr enrichment driven by the SIA flux. However, Barnard *et al.* also show that small modifications of PD migration barriers (close to the accuracy of DFT calculations) are sufficient to reverse the RIS tendencies and reproduce the experimental results. Considering that the predictions of Refs. 43 and 121 are based on DFT calculations in ferromagnetic alloys and are only valid in the dilute limit, it is, therefore, not surprising that they differ from experimental observations in concentrated and paramagnetic Ni-Cr alloys.

Finally, AKMC simulations of RIS in W–Re alloys have been performed with AKMC simulations<sup>97,122</sup> using a pair interaction model similar to the one in Ref. 24 for Fe–Cr. W is a candidate material for plasma-facing components of future fusion nuclear reactors, and transmutations produced by 14 MeV neutrons may lead to the formation of up to 0.8 at. % of Re during the lifetime of these components (and to smaller concentrations of Os and Ta). The mixed dumbbell is stable and can diffuse in 3D (whereas the pure W dumbbell is confined to a 1D motion). Vacancies are strongly bonded to Re atoms and drag them toward the sinks. Both mechanisms contribute to an enrichment of Re at GBs, in agreement with some experimental observations.<sup>97</sup> In W–Re–Os, a concentration-dependent pair interaction is used to stabilize vacancy clusters despite the fact that vacancy pairs are unstable at 0 K. The AKMC simulations show a RIS of Re and Os on cavities.<sup>122</sup> A quantitative study of RIS profiles and their analysis in relation to the thermodynamic properties of W-based alloys remain to be done.

#### IV. DYNAMICAL COUPLING BETWEEN RIS AND MICROSTRUCTURE EVOLUTION

The diffusion of PDs and their annihilation/creation reactions at sinks induce RIS but also transformations of the microstructure. PDs that eliminate on pre-existing GBs can make them slide—potentially leading to grain coarsening or creep under applied stress—or transform them into temporary reservoirs of PDs.<sup>123</sup> PDs that eliminate on dislocations can make them move by a climbing mechanism, grow or shrink when they are dislocation loops, or even transform them into a network of dislocation lines when loops are large enough to interact between them. Changes in the microstructure that are accompanied by a change in the density, size, or nature of the sinks may have a spectacular effect on RIS because the distribution of solutes between sinks is then modified. Inversely, RIS has an effect on the microstructure. The primary impact of RIS is to enhance or induce second-phase precipitation or dissolution. RIP occurs mainly on sinks following local RIS-induced enrichment in solute or in the bulk whenever the bulk composition is affected by RIS. Non-coherent precipitation induced by RIS and absorbing PDs may transform or even remove sinks.<sup>124</sup> Another effect of RIS is the modification of sink absorption efficiencies of vacancy and SIA, which may lead to significant modification of the bias for void nucleation and swelling.<sup>125</sup> These modifications of the microstructure and RIS take place in parallel. Therefore, rigorously speaking, the system never reaches a true steady-state.

As mentioned above, sink strengths may vary with time, mainly because of PD cluster evolution. One may rely on more sophisticated rate theory models than the homogeneous mean field rate theory model of Eq. (2). The cluster dynamics and OKMC methods simulate the kinetics of PD clusters. In these methods, the microstructure is modeled as a gas of isolated clusters with clusters absorbing or emitting mobile species. Generally, only isolated PDs migrate and the recombination reaction between vacancy and SIA is included. In cluster dynamics, the capture rate is deduced from the steady state flux of mobile species toward the cluster, while the emitting rate is related to the binding interaction between the

cluster and the mobile species so as to ensure detailed balance at equilibrium. A set of coupled master equations govern the evolution of clusters. In OKMC, once the event rates are known, one may simulate the stochastic kinetics of the microstructure using a residence time algorithm.

Below, we present a few examples of simulation approaches that address the kinetic couplings between RIS and the microstructure. The first two examples are about the modeling of the RIP phenomena following RIS in connection with a time-dependent microstructure, and the last examples explore the dynamic effects of an evolving heterogeneous microstructure on RIS.

#### A. RIS and RIP in a time-evolving microstructure

In an AKMC simulation method, it is possible to incorporate a-thermal events such as the production of PDs, the recombination between vacancy and SIAs, and PD annihilation on a static ideal sink with simplified geometry.<sup>82,92,113</sup> It is, thus, the appropriate method to study RIS and RIP phenomena. However, what is much more difficult to simulate are the agglomeration processes of PDs, mainly for the following three reasons:

- the limitations in size of the simulation box reduces the time of presence of several PDs in the box;
- the great challenge of simulating the formation of off-lattice defects such as dislocation loops; and
- the trapping of PDs on the lattice sites near a PD cluster that produces numerous correlated jumps and no evolution of the microstructure in the allocated CPU time.

To overcome these difficulties, recent approaches simulated the kinetics of the PD clusters separately to deduce from it a temporal evolution of the average sink strength and to include it in an AKMC simulation through the rescaling of the Monte Carlo time.<sup>113</sup>

Although RIS is not the main focus of the authors in Ref. 113, they tackle complex coupling between equilibrium segregation, the RIS of Cr on the GB, the precipitation of Cr-rich precipitates in the vicinity of a GB, and eventually the variation of PD concentration with the time-evolving microstructure. Due to the limitations in the size of the simulation box, a single GB in a Monte Carlo box already yields a sink strength that is much too high compared with realistic experimental values. Adding the effect of PD clusters on the sink strength would result in an even greater overestimation of the sink strength. However, as long as we neglect the mobility of PD clusters and assume that PDs instantaneously reach their stationary concentration values ( $X_d^{st}$ ) for a given microstructure and that mutual recombination reactions between PDs are negligible, we can directly relate the concentration of PDs to the evolution of the sink strength using Eq. (2),

$$X_d^{st} = \frac{G}{D_d k_d^2(t)}, \quad (7)$$

where at any time  $t$ ,  $k_d^2(t)$  represents the overall sink strength summing contributions from all the sinks of the microstructure. The sink strength of the AKMC simulation is the GB sink strength,  $k_d^2 = k_d^2(\text{GB})$ . In the cluster dynamics (CD), the sink strength

results from the time-dependent PD clusters,  $k_d^2(t) = k_d^2(\text{CD})$ . To reproduce these steady-state PD concentrations, one should rescale the Monte Carlo time with the following law:<sup>126</sup>

$$t = t_{\text{AKMC}} \times \frac{X_d^{\text{st}}(\text{AKMC})}{X_d^{\text{st}}(\text{CD})} = t_{\text{AKMC}} \times \frac{k_d^2(\text{CD})}{k_d^2(\text{GB})}, \quad (8)$$

where  $t_{\text{AKMC}}$  is the Monte Carlo residence time. This law stems from the assumption that RED is linear in PD concentrations, and therefore, a higher PD concentration leads to faster kinetics. From Eq. (7), the ratio of concentrations can be expressed as the ratio of sink strengths as long as PD kinetics is dominated by the elimination of PDs at sinks. Note that to keep a unique definition of the time, one should neglect the sink biases, which is equivalent to imposing  $k_V^2 = k_I^2 = k^2$ . Another way of dealing with the evolution of the sink densities and point defect concentrations during irradiation has been proposed in Ref. 127 (but not yet applied to RIS). As in the previous case, CD is first used to estimate the evolution of the sink strength. A random distribution of point-like PD sinks is introduced in AKMC simulations, with the same sink strength. The advantage of the methods is that the simulations are performed with real PD concentrations and, therefore, with the real ratio between SIA and V, and the correct competition between recombination and annihilations at sinks. In principle, the introduction of elastic interactions between the sinks and PDs would give access to the effects of a biased sink on RIS, something that cannot be done with the simple time rescaling method of Eq. (8).

Note that in these two studies, the authors rely on a rate theory CD with parameters adjusted to simulate the radiation-induced microstructure in pure Fe.<sup>113,127</sup> Explicitly taking into account the alloying effects on the capture and emission rates is a challenging task, especially in concentrated alloys and even more so if we want to include the effects of RIS on these rates. Cluster dynamics simulations predict that the dominant sink is the pre-existing dislocation network at the beginning of irradiation and then the vacancy clusters formed in displacement cascades at longer times or doses. The transposition of the simulated microstructure into the variation in time of an average sink strength could yield a quantitative modeling of coupling between RED, RIS, and RIP, as illustrated in Fig. 6.<sup>113</sup>

In a second example, cluster dynamics is not used to simulate the kinetics of PD clusters, but the clustering of solute atoms leading to heterogeneous precipitation of Mn–Ni–Si precipitates (MNSPs) in a ferro-martensitic steel.<sup>128</sup> The RIS and heterogeneous precipitation are assumed to occur on an immobile dislocation line. The dislocation line is both a PD sink and a reservoir of heterogeneous nucleation sites. The RIS resulting from the elimination of PDs on the dislocation is deduced from the numerical solution to phenomenological diffusion equations accounting for PD-solute flux couplings such as the ones of Eq. (1). By increasing the solute concentration on the sink, RIS magnifies or even produces a local precipitation driving force. This thermodynamic driving force is explicitly included in the emitting rate of the mobile species in this cluster dynamics method.<sup>128</sup>

The main conclusion of this work was that the positive RIS of Si and Ni is a necessary step toward heterogeneous precipitation of

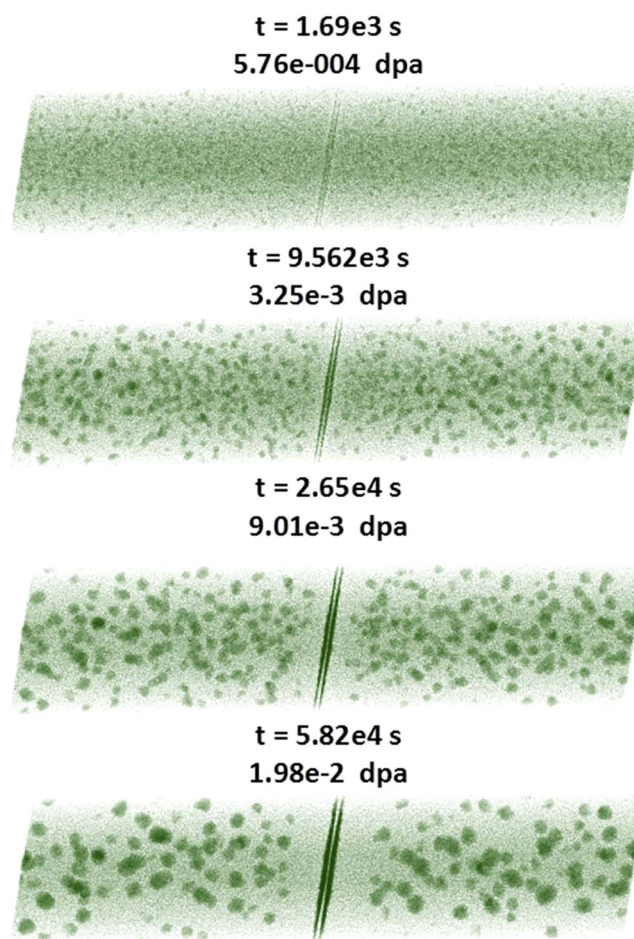


**FIG. 6.** AKMC simulations of  $\alpha$ - $\alpha'$  phase separation in Fe-15 at. % Cr under an irradiation at 290 °C and  $3.4 \times 10^{-7}$  dpa  $s^{-1}$ , with a negative segregation energy of Cr on the GB and on the neighboring planes, leading to the equilibrium segregation of Cr on the GB.<sup>113</sup> Reproduced with permission from Soisson and Jourdan, *Acta Mater.* **103**, 870 (2016). Copyright 2016 Elsevier.

MNSPs in an undersaturated stable matrix because it provides both a reservoir of solutes, interfacial dislocations, and a catalytic effect driven by the removal of the dislocation core.<sup>128</sup> As emphasized by the authors, the RIS model is extremely simplified and should rather be seen as an interpolation scheme introduced to reproduce the variation of solute enrichment from 0 to 7 dpa measured by Jiao and Was at various PD sinks.<sup>129</sup> Consistencies between the RIS and cluster dynamics models could also be improved:

- the RED model that fixes the absorption rates of the solute clusters is not consistent with the RIS model because the segregation profile of PDs nearby the dislocation should affect RED; and
- the depletion of solutes in the matrix due to RIS-induced enrichment of solutes on the sink is ignored, while it may reduce the RIS solute fluxes and change the bulk population of PD-solute

clusters. This effect has been highlighted and simulated by deriving DFT-based flux coupling coefficients and rate theory models of the impact of RIS on the bulk properties of PD-solute clusters in dilute solid solutions.<sup>130</sup>

Besides, RIS occurs on every sinks, in particular, on the PD clusters and interfaces of non-coherent precipitates. Up to now, there is no cluster dynamics methods accounting for these coupled kinetic mechanisms.

To conclude, the next challenge of this cluster dynamics approach is the consistent modeling of the concurrent PD and solute clustering reactions in a spatially resolved RIS profile. This would imply to solve spatially dependent coupled master equations for every PD and solute clusters of the microstructure in a self-consistent way, including the concentration of mobile solutes and PDs. Note that in principle, the kinetic phenomena investigated by this cluster dynamics method could have been simulated by the previously presented AKMC method, provided non-coherent precipitation can be approximated by an on-lattice precipitation mechanism. Nevertheless, even if the precipitates were coherent, the possibility of extending the cluster dynamics method to the modeling of concurrent second-phase precipitation and PD cluster formation fully justifies the developments of this mesoscopic approach because it is much more efficient than the AKMC method and, therefore, allows to model larger time- and length-scales.

## B. RIS in a space- and time-evolving heterogeneous microstructure

A heterogeneous microstructure produces complex redistribution mechanisms of the alloying elements. For instance, Huang *et al.* have shown that the distribution in size and position of the dislocation loops observed by transmission electron microscopy mostly determines the distribution of RIS on individual sinks and local bulk compositions in between sinks.<sup>88</sup> From a DFT-based calculation of flux coupling coefficients and a finite-difference solution to the resulting PD and solute diffusion equations, Huang *et al.* deduce the steady-state RIS profile within a given Voronoi's volume occupied by a single loop. From a statistical sampling of the Voronoi's volume and the dislocation loop radius modeled after the characterization of the microstructure by transmission electron microscopy, the full RIS distribution is obtained. In the dilute Ni-Ti alloy, the resulting RIS distribution is in quantitative agreement with direct atom probe tomography measurements of local Ti composition distributions.

It was also shown that RIS in nanocrystalline and coarse-grained materials can be very different. The reason is twofold: (a) RIS on GBs decreases linearly with decreasing grain size as already shown in Ref. 82; (b) in polycrystals, the bulk composition of a grain was observed to depend on its size and surrounding grains, which in turn affects RIS.<sup>119</sup> We believe that this grain-level redistribution is driven by the difference in the fluxes of PDs between grains. Indeed, for a steady state to be reached, fluxes of atomic species on both sides of the GB must be balanced. The greater flux of PDs in smaller grains leads to higher atomic fluxes toward or away from the GB. One way to reduce these atomic fluxes, is either to reduce or increase the bulk concentration of, respectively, the depleted and enriched alloying elements.

Interestingly, under dynamic conditions of grain-coarsening, the bulk solute redistribution between grains is radically opposite to the one of a frozen microstructure. This result was obtained by running two PF simulations in parallel, the first one simulating the thermal grain coarsening and the second one simulating RIS of the time-dependent coarsened-grain microstructure.<sup>119</sup> As shown in Fig. 7, the slide of GBs occurs faster than the RIS relaxation kinetics, leaving behind a depleted area in alloying elements with negative RIS. Since the small grains grow at the expense of large grains, the outward motion of GBs leave depleted areas that tend to decrease the average concentrations of the small grain in depleted alloying elements. The same mechanism explains the formation of asymmetrical RIS profiles with higher concentration in the larger grain, as it was observed experimentally,<sup>131</sup> and simulated by previous 1D kinetic models.<sup>132</sup> These mesoscopic simulations highlight the importance of a dynamic approach to investigate the RIS-microstructure interplay.

The same PF method could be extended to the simulation of several PD sink population, as it was proposed in the hybrid PF-cluster dynamics method of Badillo *et al.*<sup>95</sup> However, this approach does not account for solute drag by GB motion, the effect of the elimination of PDs and RIS on the mobility of the GB and the resulting change of the grain structure. Yet, kinetic phenomena such as radiation-induced diffusional creep imply a non-symmetric creation and annihilation of PDs at sinks leading to the motion of PD sinks. This is a case where the GB motion is not due to thermal grain growth but to the elimination of radiation-induced PDs at the GB.

Another application of the PF method to problems of microstructure-RIS dynamic interplays was the core mobility of a dislocation and its surrounding RIS.<sup>133,133</sup> The dislocation climbs because of the preferential absorption of SIAs by the dislocation core. The authors control the bias between vacancy and SIA elimination rates on dislocation through the addition of a neutral and immobile sink in PF simulation,<sup>133</sup> or through an effective sink strength,  $k_c^2$ , modeling the influence of the surrounding microstructure on the PD elimination rates.<sup>133</sup> Note that the standard assumption of perfect sinks could be alleviated thanks to an explicit modeling of PD elimination mechanisms at dislocation jogs. The fluxes of chemical species coupled to the PD fluxes toward the dislocation lead to RIS. RIS was studied in the Fe-11 at. % Cr alloy at  $T = 700$  K on a dislocation loop simulated by a 2D edge dislocation dipole<sup>133</sup> and also on a small angle GB simulated by a piling of dislocations.<sup>133</sup> The flux of SIAs toward the tensile regions of dislocation is dominant over the vacancy one, leading to an enrichment in Cr, while the flux of vacancies toward the region in compression is the dominant one, leading to depletion in Cr. Though the variation of the effective sink strength is slightly non-monotonous, the climb rate globally increases with decreasing neutral effective sink strength,  $k_c^2$ , because the PD bulk concentrations and corresponding fluxes increase with decreasing  $k_c^2$ . The higher the climb rate, the wider the RIS profile and the smaller the Cr depletion in the regions in compression. This is because, in the climbing process, the compressive regions gaining on the tensile region are initially enriched in Cr. Then, the climbing rate is fast enough to inhibit the RIS-assisted depletion of Cr in newly compressive regions.

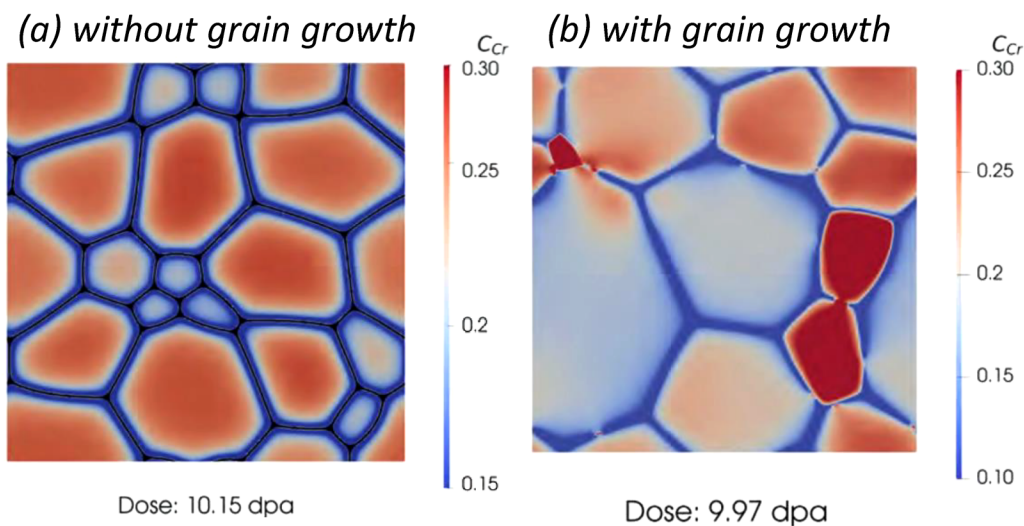


**FIG. 7.** PF modeling of the Cr concentration field ( $C_{Cr}$ ) in a Fe-Ni-Cr polycrystalline alloy.<sup>119</sup> Temperature is set to  $T = 673$  K, the irradiation dose rate to  $G = 10^{-6}$  dpa/s and the dose is equal to (a) 10.5 and (b) 9.97 dpa. GBs correspond to the regions with depleted Cr (in blue). Figure (a) shows a RIS simulation in a frozen polycrystal grain structure and (b) a simulation result of concurrent GB migration and RIS. Reproduced with permission from Rezwan *et al.*, *J. Nucl. Mater.* **563**, 153 614 (2022). Copyright 2022 Elsevier.

Such interplay may drastically change the variation of RIS with temperature, radiation dose rate, and microstructure sink strength. For instance, in the kinetic regime dominated by the elimination of PDs at sinks, we do not expect a strong variation of RIS with the PD bulk concentration,<sup>9</sup> while RIS may vary due to the PD concentration-dependent climbing rate. However, as emphasized by the authors, the numerous parameters of a multi-physics PF method with strongly coupled physical phenomena are difficult to determine, especially the ones associated with the complex mobility mechanism of dislocation.

## V. OPEN QUESTIONS

This final part of the paper is devoted to the discussion of some important still open questions and a brief comment on promising approaches for the near future. Through several examples of recent works in the field of RIS, we have shown how a rigorous combination of modelling tools at various time and length scales provides relevant insights into this complex phenomenon.

At the foundation of this multi-scale modeling approach lie *ab initio* calculations of PD-solute interaction energies and migration barriers. We have already discussed the numerous leads of improvement on this topic, with the aim to represent more and more faithfully the energetic landscape of a system: temperature effects, magnetic excitations, and stress/strain contributions to name a few.

But databases of DFT calculations alone do not provide any useful information to characterize RIS, and there is a crucial need for analytical and numerical models that are able to compute the Onsager matrix of a system from the energetic landscape. This coarse-graining step is essential to address the physics of RIS. Promising works are underway in this direction, and it will most certainly open a whole set of new modeling capacities in the near future.

Let us stress that results obtained for dilute alloys cannot be readily extrapolated to concentrated alloys. More work is required on concentrated alloys to develop models that will guide the construction of DFT databases because for these alloys the phase space is obviously too large to be studied comprehensively. The soaring interest in the so-called high-entropy alloys is a nice opportunity to develop our modeling capabilities for concentrated alloys. Among concentrated alloys, austenitic stainless steels must be highlighted because of their importance in the nuclear industry. Yet, these alloys are concentrated, multi-components and paramagnetic, and each one of these three characteristics produces specific modeling issues.

The modeling of RIS being intrinsically multi-scale, the question of uncertainty propagation arises naturally. One advantage of analytical models over numerical simulations (e.g., AKMC) is that they allow for efficient studies of the sensitivity of the outputs with respect to uncertainties in the inputs. It can happen that predicted flux coupling tendencies are very sensitive to the values of binding and migration energies computed by DFT. In this respect, the study of uncertainty propagation throughout kinetic models is a necessary tool to identify such cases and if possible provide additional work to increase the reliability of the results.

Once the transport coefficients are known, the next step is to model the diffusion of solutes and PDs around a given PD sink. Recent works focused on taking into account the effect of the strain field around a sink (e.g., dislocation, GB) on the reaction-diffusion equations. This is obviously a key step, but there are other details that, in our opinion, have been somehow overlooked so far. First of all, the simultaneous consideration of thermodynamic segregation and RIS at sinks. The interplay between both is well-known, and the W-shaped RIS profiles are the most prominent examples of this interplay (these profiles observed, e.g., for Cr at

grain-boundaries in austenitic steels, occur when the thermodynamic segregation is positive while RIS is negative<sup>134</sup>). But both phenomena are often not quantified simultaneously. The reason is that thermodynamic segregation requires the atomic details of the sink while RIS is usually assumed to be limited by diffusion away from the sink, and therefore, the sink may be crudely modeled by a PD capture radius with a given boundary condition. The rigorous definition of this capture radius and the associated boundary condition is another question of uttermost importance, which relates to the coarse-graining of the atomic diffusion model near the sink. Generally speaking, boundary conditions in diffusion problems have a tendency to hide critical approximations, and one must be very thoughtful and cautious when setting up these conditions.

These two items (sink capture radius and equilibrium segregation) can be naturally accounted for in atomic scale simulations such as AKMC, but these simulations provide insights into a limited space and time scale only. As we shall explain shortly, this insight is generally not sufficient.

For both atomic models and models based on continuous diffusion equations, the parameterization of the irradiation source term deserves some attention because it is generally assumed that irradiation produces only isolated PDs and small PD clusters and that the interaction with solutes occurs during the course of PD diffusion. Recent molecular studies of displacement cascades seem to show that the small PD-solute cluster may also form during the cascade, with distributions that may (or may not) be different from the ones expected from local equilibrium assumptions. If this is confirmed, it will most probably affect RIS profiles.

Finally, we believe that it is crucial to acknowledge the fact that RIS depends on the surrounding sink microstructure and that this microstructure must be thought of as a whole and not as a collection of individual sinks. Most importantly, the sink microstructure evolves under irradiation and RIS plays a role in this evolution. Therefore, the interplay between RIS and sink microstructure is dynamical, and this changes everything in the way we must establish modeling strategies for this phenomenon. An analytical RIS model accounting for the dynamics of the sink is highly desirable—even if it is limited to simple cases only—to answer basic questions such as the conditions under which it is correct to assume that RIS establishes much more quickly than the sink structure evolves.

Knowing that, microstructural information (local sink densities and size distributions) is required when comparing modeling with experiments or even two sets of experimental data. We know very little about how exactly solute and PD redistribution affect the structure of sinks and vice versa, even though a large number of well-studied phenomena are involved: interface complexion, heterogeneous precipitation (coherent, semi-coherent, or incoherent), the change of GB structure upon segregation, grain growth, dislocation climbing, solute drag by interface mobility, etc. All these changes in the sink structure are likely to modify the vacancy/SIA sink absorption bias and therefore the RIS itself and therefore the kinetics of sink evolution. Due to this dynamical interplay, we should aim at modeling the RIS phenomenon at microstructure scale. Let us end this paragraph with an enlightening example on this matter: in the sink elimination regime, RIS has been shown not to depend on the absolute values of PD concentrations. If the sink microstructure is

stationary, the RIS width depends on temperature only; if the number of sinks increases (for instance, due to PD clustering), RIS diminishes as solutes must redistribute among a larger sink population; if the number of sinks decreases, RIS will also increase around each sink, eventually leading to RIP, and the precipitates themselves may act as very efficient PD sinks, thereby re-increasing the number of sinks.

We believe that a coupling between cluster dynamics and PF methods parameterized by atomic-scale data is currently the most promising approach to obtain a comprehensive modeling of the RIS phenomenon. Indeed, cluster dynamics allows a correct treatment of PD and solute clustering, while PF naturally accounts for spatial correlations between sinks, elasticity fields, the details of solute and PD concentration fields, and interface (or sink) mobility. The scale at which this coupling must be performed remains a question to be treated rigorously, and numerical progress in solving PF equations for fairly large 3D systems (i.e., large enough to represent a relevant local sink population) is also required to provide meaningful comparison with experimental results because most PF simulations are currently limited to the 2D system to obtain a decent computational load. One must also bear in mind that as we increase the complexity of the RIS model by adding more and more simultaneous physical phenomena to it, the number of model parameters increases as well, and some of these parameters are more or less arbitrary and difficult to evaluate rigorously. Ensuring that the predicted RIS does not depend on these somehow artificial parameters is obviously a key to obtain a trustful predictive modeling of RIS.

## AUTHOR DECLARATIONS

### Conflict of Interest

The authors have no conflicts to disclose.

### Author Contributions

**T. Schuler:** Conceptualization (equal); Investigation (equal); Methodology (equal); Writing – original draft (equal); Writing – review & editing (equal). **M. Nastar:** Conceptualization (equal); Investigation (equal); Methodology (equal); Writing – original draft (equal); Writing – review & editing (equal). **F. Soisson:** Conceptualization (equal); Investigation (equal); Methodology (equal); Writing – original draft (equal); Writing – review & editing (equal).

### DATA AVAILABILITY

Data sharing is not applicable to this article as no new data were created or analyzed in this study.

## REFERENCES

- <sup>1</sup>K. Russell, “Phase stability under irradiation,” *Prog. Mater. Sci.* **28**, 229–434 (1984).
- <sup>2</sup>G. Was, *Fundamentals of Radiation Materials Science* (Springer, New York, 2017).
- <sup>3</sup>T. Anthony, “Solute segregation in vacancy gradients generated by sintering and temperature changes,” *Acta Metall.* **17**, 603–609 (1969).

- <sup>4</sup>P. Okamoto and H. Wiedersich, "Segregation of alloying elements to free surfaces during irradiation," *J. Nucl. Mater.* **53**, 336–345 (1974).
- <sup>5</sup>E. Marquis and R. H. T. Rousseau, "A systematic approach for the study of radiation-induced segregation/depletion at grain boundaries in steels," *J. Nucl. Mater.* **413**, 1–4 (2011).
- <sup>6</sup>Q. Chen, R. Hu, S. Jin, F. Xue, and G. Sha, "Irradiation-induced segregation/desegregation at grain boundaries of a ferritic Fe-Mn-Si steel," *Acta Mater.* **220**, 117297 (2021).
- <sup>7</sup>T. G. Lach, M. J. Olszta, S. D. Taylor, K. H. Yano, D. J. Edwards, T. S. Byun, P. H. Chou, and D. K. Schreiber, "Correlative STEM-APT characterization of radiation-induced segregation and precipitation of in-service BWR 304 stainless steel," *J. Nucl. Mater.* **549**, 152894 (2021).
- <sup>8</sup>Q. Barrès, O. Tissot, E. Meslin, I. Mouton, B. Arnal, M. Loyer-Prost, and C. Pareige, "Effect of grain boundary planes on radiation-induced segregation (RIS) at near  $\Sigma 3$  grain boundaries in Fe-Cr alloy under ion irradiation," *Mater. Charact.* **184**, 111676 (2022).
- <sup>9</sup>L. Huang, M. Nastar, T. Schuler, and L. Messina, "Multiscale modeling of the effects of temperature, radiation flux, and sink strength on point-defect and solute redistribution in dilute Fe-based alloys," *Phys. Rev. Mater.* **5**, 033605 (2021).
- <sup>10</sup>L. Onsager, "Reciprocal relations in irreversible processes. I," *Phys. Rev.* **37**, 405–426 (1931).
- <sup>11</sup>L. Onsager, "Reciprocal relations in irreversible processes. II," *Phys. Rev.* **38**, 2265–2279 (1931).
- <sup>12</sup>R. Sizmann, "The effect of radiation upon diffusion in metals," *J. Nucl. Mater.* **69–70**, 386–412 (1978).
- <sup>13</sup>A. Ardell and P. Bellon, "Radiation-induced solute segregation in metallic alloys," *Curr. Opin. Solid State Mater. Sci.* **20**, 115–139 (2016).
- <sup>14</sup>M. Nastar and F. Soisson, "1.08—radiation-induced segregation," in *Comprehensive Nuclear Materials*, 2nd ed., edited by R. J. Konings and R. E. Stoller (Elsevier, Oxford, 2020), pp. 235–264.
- <sup>15</sup>X. Wang, H. Zhang, T. Baba, H. Jiang, C. Liu, Y. Guan, O. Elleuch, T. Kuech, D. Morgan, J.-C. Idrobo, P. M. Voyles, and I. Szlufarska, "Radiation-induced segregation in a ceramic," *Nat. Mater.* **19**, 992–998 (2020).
- <sup>16</sup>A. J. Samin, D. A. Andersson, E. F. Holby, and B. P. Uberuaga, "On the role of electro-migration in the evolution of radiation damage in nanostructured ionic materials," *Electrochem. Commun.* **96**, 47–52 (2018).
- <sup>17</sup>A. Allnatt, "Einstein and linear response formulae for the phenomenological coefficients for isothermal matter transport in solids," *J. Phys. C: Solid State Phys.* **15**, 5605–5613 (1982).
- <sup>18</sup>M. R. Sorensen and A. F. Voter, "Temperature-accelerated dynamics for simulation of infrequent events," *J. Chem. Phys.* **112**, 9599–9606 (2000).
- <sup>19</sup>A. F. Voter, F. Montalenti, and T. C. Germann, "Extending the time scale in atomistic simulation of materials," *Annu. Rev. Mater. Res.* **32**, 321–346 (2002).
- <sup>20</sup>D. Perez, B. P. Uberuaga, and A. F. Voter, "The parallel replica dynamics method—coming of age," *Comput. Mater. Sci.* **100**, 90–103 (2015).
- <sup>21</sup>T. D. Swinburne and D. Perez, "Self-optimized construction of transition rate matrices from accelerated atomistic simulations with bayesian uncertainty quantification," *Phys. Rev. Mater.* **2**, 053802 (2018).
- <sup>22</sup>V. Pechenkin, V. Molodtsov, V. Ryabov, and D. Terentyev, "On the radiation-induced segregation: Contribution of interstitial mechanism in Fe-Cr alloys," *J. Nucl. Mater.* **433**, 372–377 (2013).
- <sup>23</sup>L. Barnard and D. Morgan, "Ab initio molecular dynamics simulation of interstitial diffusion in Ni-Cr alloys and implications for radiation induced segregation," *J. Nucl. Mater.* **449**, 225–233 (2014).
- <sup>24</sup>O. Senninger, F. Soisson, E. Martínez, M. Nastar, C.-C. Fu, and Y. Bréchet, "Modeling radiation induced segregation in iron-chromium alloys," *Acta Mater.* **103**, 1–11 (2016).
- <sup>25</sup>B. Puchala, M. Falk, and K. Garikipati, "An energy basin finding algorithm for kinetic Monte Carlo acceleration," *J. Chem. Phys.* **132**, 134104 (2010).
- <sup>26</sup>M. Athènes and V. Bulatov, "Path factorization approach to stochastic simulations," *Phys. Rev. Lett.* **113**, 230601 (2014).
- <sup>27</sup>C. Daniels and P. Bellon, "Hybrid kinetic Monte Carlo algorithm for strongly trapping alloy systems," *Comput. Mater. Sci.* **173**, 109386 (2020).
- <sup>28</sup>K. Ferasat, Y. N. Osetsky, A. V. Barashev, Y. Zhang, Z. Yao, and L. K. Béland, "Accelerated kinetic Monte Carlo: A case study; vacancy and dumbbell interstitial diffusion traps in concentrated solid solution alloys," *J. Chem. Phys.* **153**, 074109 (2020).
- <sup>29</sup>B. P. Uberuaga, E. Martínez, D. Perez, and A. F. Voter, "Discovering mechanisms relevant for radiation damage evolution," *Comput. Mater. Sci.* **147**, 282–292 (2018).
- <sup>30</sup>Y. N. Osetsky, L. K. Béland, and R. E. Stoller, "Specific features of defect and mass transport in concentrated fcc alloys," *Acta Mater.* **115**, 364–371 (2016).
- <sup>31</sup>A. Ervin and H. Xu, "Mesoscale simulations of radiation damage effects in materials: A SEAKMC perspective," *Comput. Mater. Sci.* **150**, 180–189 (2018).
- <sup>32</sup>M. Trochet, N. Mousseau, L. K. Béland, and G. Henkelman, "Off-lattice kinetic monte carlo methods," in *Handbook of Materials Modeling* (Springer International Publishing, 2020), pp. 715–743.
- <sup>33</sup>D. Trinkle, "Automatic numerical evaluation of vacancy-mediated transport for arbitrary crystals: Onsager coefficients in the dilute limit using a Green function approach," *Philos. Mag.* **97**, 2514–2563 (2017).
- <sup>34</sup>T. Schuler, L. Messina, and M. Nastar, "KineClue: A kinetic cluster expansion code to compute transport coefficients beyond the dilute limit," *Comput. Mater. Sci.* **172**, 109191 (2020).
- <sup>35</sup>M. Nastar, V. Y. Dobretsov, and G. Martin, "Self-consistent formulation of configurational kinetics close to equilibrium: The phenomenological coefficients for diffusion in crystalline solids," *Philos. Mag. A* **80**, 155 (2000).
- <sup>36</sup>R. Agarwal and D. R. Trinkle, "Ab initio magnesium-solute transport database using exact diffusion theory," *Acta Mater.* **150**, 339–350 (2018).
- <sup>37</sup>A. C. P. Jain, P. A. Burr, and D. R. Trinkle, "First-principles calculations of solute transport in zirconium: Vacancy-mediated diffusion with metastable states and interstitial diffusion," *Phys. Rev. Mater.* **3**, 033402 (2019).
- <sup>38</sup>L. Messina, M. Nastar, T. Garnier, C. Domain, and P. Olsson, "Exact ab initio transport coefficients in bcc Fe-X (X=Cr, Cu, Mn, Ni, P, Si) dilute alloys," *Phys. Rev. B* **90**, 104203 (2014).
- <sup>39</sup>L. Messina, M. Nastar, N. Sandberg, and P. Olsson, "Systematic electronic-structure investigation of substitutional impurity diffusion and flux coupling in bcc iron," *Phys. Rev. B* **93**, 184302 (2016).
- <sup>40</sup>H. Wu, T. Mayeshiba, and D. Morgan, "High-throughput ab-initio dilute solute diffusion database," *Sci. Data* **3**, 160054 (2016).
- <sup>41</sup>T. Schuler, P. Bellon, D. R. Trinkle, and R. S. Averback, "Modeling the long-term evolution of dilute solid solutions in the presence of vacancy fluxes," *Phys. Rev. Mater.* **2**, 073605 (2018).
- <sup>42</sup>L. Messina, T. Schuler, M. Nastar, M.-C. Marinica, and P. Olsson, "Solute diffusion by self-interstitial defects and radiation-induced segregation in ferritic Fe-X (X=Cr, Cu, Mn, Ni, P, Si) dilute alloys," *Acta Mater.* **191**, 166–185 (2020).
- <sup>43</sup>E. Toijer, L. Messina, C. Domain, J. Vidal, C. S. Becquart, and P. Olsson, "Solute-point defect interactions, coupled diffusion, and radiation-induced segregation in fcc nickel," *Phys. Rev. Mater.* **5**, 013602 (2021).
- <sup>44</sup>J. Tucker, R. Najafabadi, T. Allen, and D. Morgan, "Ab initio-based diffusion theory and tracer diffusion in Ni-Cr and Ni-Fe alloys," *J. Nucl. Mater.* **405**, 216–234 (2010).
- <sup>45</sup>S. Choudhury, L. Barnard, J. Tucker, T. Allen, B. Wirth, M. Asta, and D. Morgan, "Ab-initio based modeling of diffusion in dilute bcc Fe-Ni and Fe-Cr alloys and implications for radiation induced segregation," *J. Nucl. Mater.* **411**, 1–14 (2011).
- <sup>46</sup>C. Becquart, R. N. Happy, P. Olsson, and C. Domain, "A DFT study of the stability of SIAs and small SIA clusters in the vicinity of solute atoms in Fe," *J. Nucl. Mater.* **500**, 92–109 (2018).
- <sup>47</sup>T. Schuler, M. Nastar, and L. Messina, "Mass-transport properties of ternary Fe(C, O) alloys revealed by multicomponent cluster synergies," *Phys. Rev. Mater.* **4**, 020401(R) (2020).
- <sup>48</sup>A. J. Samin, D. A. Andersson, E. F. Holby, and B. P. Uberuaga, "Ab initio based examination of the kinetics and thermodynamics of oxygen in Fe-Cr alloys," *Phys. Rev. B* **99**, 174202 (2019).

- <sup>49</sup>K. Jin and H. Bei, "Single-phase concentrated solid-solution alloys: Bridging intrinsic transport properties and irradiation resistance," *Front. Mater.* **5**, 1 (2018).
- <sup>50</sup>O. El-Atwani, N. Li, M. Li, A. Devaraj, J. K. S. Baldwin, M. M. Schneider, D. Sobieraj, J. S. Wróbel, D. Nguyen-Manh, S. A. Maloy, and E. Martinez, "Outstanding radiation resistance of tungsten-based high-entropy alloys," *Sci. Adv.* **5**, eaav2002 (2019).
- <sup>51</sup>M. A. Cusentino, M. A. Wood, and R. Dingreville, "Compositional and structural origins of radiation damage mitigation in high-entropy alloys," *J. Appl. Phys.* **128**, 125904 (2020).
- <sup>52</sup>M. Mizuno, K. Sugita, and H. Araki, "Defect energetics for diffusion in CrMnFeCoNi high-entropy alloy from first-principles calculations," *Comput. Mater. Sci.* **170**, 109163 (2019).
- <sup>53</sup>X. Zhang, S. V. Divinski, and B. Grabowski, "Ab initio prediction of vacancy energetics in HCP Al-Hf-Sc-Ti-Zr high entropy alloys and the subsystems," *Acta Mater.* **227**, 117677 (2022).
- <sup>54</sup>S. L. Thomas and S. Patala, "Vacancy diffusion in multi-principal element alloys: The role of chemical disorder in the ordered lattice," *Acta Mater.* **196**, 144–153 (2020).
- <sup>55</sup>C. M. Barr, G. A. Vetterick, K. A. Unocic, K. Hattar, X.-M. Bai, and M. L. Taheri, "Anisotropic radiation-induced segregation in 316L austenitic stainless steel with grain boundary character," *Acta Mater.* **67**, 145–155 (2014).
- <sup>56</sup>C. M. Barr, L. Barnard, J. E. Nathaniel, K. Hattar, K. A. Unocic, I. Szlurfarska, D. Morgan, and M. L. Taheri, "Grain boundary character dependence of radiation-induced segregation in a model Ni-Cr alloy," *J. Mater. Res.* **30**, 1290–1299 (2015).
- <sup>57</sup>J. Zhang, H. He, W. Liu, L. Kang, D. Yun, and P. Chen, "Effects of grain boundaries on the radiation-induced defects evolution in BCC Fe-Cr alloy: A molecular dynamics study," *Nucl. Mater. Energy* **22**, 100726 (2020).
- <sup>58</sup>P. H. Dederichs and K. Schroeder, "Anisotropic diffusion in stress fields," *Phys. Rev. B* **17**, 2524–2536 (1978).
- <sup>59</sup>C. Varvenne, F. Bruneval, M.-C. Marinica, and E. Clouet, "Point defect modeling in materials: Coupling ab initio and elasticity approaches," *Phys. Rev. B* **88**, 134102 (2013).
- <sup>60</sup>D. R. Trinkle, "Diffusivity and derivatives for interstitial solutes: Activation energy, volume, and elastodiffusion tensors," *Philos. Mag.* **96**, 2714–2735 (2016).
- <sup>61</sup>E. Clouet, C. Varvenne, and T. Jourdan, "Elastic modeling of point-defects and their interaction," *Comput. Mater. Sci.* **147**, 49–63 (2018).
- <sup>62</sup>L. Casillas-Trujillo, A. S. Ervin, L. Xu, A. Barashev, and H. Xu, "Dynamics of interaction between dislocations and point defects in bcc iron," *Phys. Rev. Mater.* **2**, 103604 (2018).
- <sup>63</sup>V. Jansson, L. Malerba, A. De Backer, C. Becquart, and C. Domain, "Sink strength calculations of dislocations and loops using OKMC," *J. Nucl. Mater.* **442**, 218–226 (2013).
- <sup>64</sup>A. Vattré, T. Jourdan, H. Ding, M.-C. Marinica, and M. Demkowicz, "Non-random walk diffusion enhances the sink strength of semicoherent interfaces," *Nat. Commun.* **7**, 10424 (2016).
- <sup>65</sup>D. Carpentier, T. Jourdan, Y. Le Bouar, and M.-C. Marinica, "Effect of saddle point anisotropy of point defects on their absorption by dislocations and cavities," *Acta Mater.* **136**, 323–334 (2017).
- <sup>66</sup>H. Rouchette, L. Thuinet, A. Legris, A. Ambard, and C. Domain, "Influence of shape anisotropy of self-interstitials on dislocation sink efficiencies in Zr: Multiscale modeling," *Phys. Rev. B* **90**, 014104 (2014).
- <sup>67</sup>H. Rouchette, L. Thuinet, A. Legris, A. Ambard, and C. Domain, "Quantitative phase field model for dislocation sink strength calculations," *Comput. Mater. Sci.* **88**, 50–60 (2014).
- <sup>68</sup>H. Rouchette, L. Thuinet, A. Legris, A. Ambard, and C. Domain, "Numerical evaluation of dislocation loop sink strengths: A phase-field approach," *Nucl. Instrum. Meth. Phys. Res. Sec. B: Beam Interact. Mater. Atoms* **352**, 31–35 (2015).
- <sup>69</sup>G. F. Bouobda Moladje, L. Thuinet, C. Domain, C. S. Becquart, and A. Legris, "Phase-field calculations of sink strength in Al, Ni, and Fe: A detailed study of elastic effects," *Comput. Mater. Sci.* **183**, 109905 (2020).
- <sup>70</sup>Z. Li and D. R. Trinkle, "Mesoscale modeling of vacancy-mediated Si segregation near an edge dislocation in Ni under irradiation," *Phys. Rev. B* **95**, 144107 (2017).
- <sup>71</sup>J. S. Wróbel, M. R. Zemla, D. Nguyen-Manh, P. Olsson, L. Messina, C. Domain, T. Wejrzanowski, and S. L. Dudarev, "Elastic dipole tensors and relaxation volumes of point defects in concentrated random magnetic Fe-Cr alloys," *Comput. Mater. Sci.* **194**, 110435 (2021).
- <sup>72</sup>X. Zhang, B. Grabowski, T. Hickel, and J. Neugebauer, "Calculating free energies of point defects from ab initio," *Comput. Mater. Sci.* **148**, 249–259 (2018).
- <sup>73</sup>G. H. Vineyard, "Frequency factors and isotope effects in solid state rate processes," *J. Phys. Chem. Solids* **3**, 121–127 (1957).
- <sup>74</sup>T. Garnier, V. R. Manga, D. R. Trinkle, M. Nastar, and P. Bellon, "Stress-induced anisotropic diffusion in alloys: Complex Si solute flow near a dislocation core in Ni," *Phys. Rev. B* **88**, 134108 (2013).
- <sup>75</sup>C. Lapointe, T. D. Swinburne, L. Thiry, S. Mallat, L. Provaille, C. S. Becquart, and M.-C. Marinica, "Machine learning surrogate models for prediction of point defect vibrational entropy," *Phys. Rev. Mater.* **4**, 063802 (2020).
- <sup>76</sup>A. Glensk, B. Grabowski, T. Hickel, and J. Neugebauer, "Breakdown of the Arrhenius law in describing vacancy formation energies: The importance of local anharmonicity revealed by ab initio thermodynamics," *Phys. Rev. X* **4**, 011018 (2014).
- <sup>77</sup>T. D. Swinburne, "Uncertainty and anharmonicity in thermally activated dynamics," *Comput. Mater. Sci.* **193**, 110256 (2021).
- <sup>78</sup>T. D. Swinburne and M.-C. Marinica, "Unsupervised calculation of free energy barriers in large crystalline systems," *Phys. Rev. Lett.* **120**, 135503 (2018).
- <sup>79</sup>A. Schneider, C.-C. Fu, F. Soisson, and C. Barreteau, "Atomic diffusion in  $\alpha$ -iron across the curie point: An efficient and transferable ab initio-based modeling approach," *Phys. Rev. Lett.* **124**, 215901 (2020).
- <sup>80</sup>A. Schneider, C.-C. Fu, O. Waseda, C. Barreteau, and T. Hickel, "Ab initio based models for temperature-dependent magnetochemical interplay in bcc Fe-Mn alloys," *Phys. Rev. B* **103**, 024421 (2021).
- <sup>81</sup>H. Wiedersich, P. Okamoto, and N. Lam, "A theory of radiation-induced segregation in concentrated alloys," *J. Nucl. Mater.* **83**, 98–108 (1979).
- <sup>82</sup>E. Martínez, O. Senninger, A. Caro, F. Soisson, M. Nastar, and B. P. Uberuaga, "Role of sink density in nonequilibrium chemical redistribution in alloys," *Phys. Rev. Lett.* **120**, 106101 (2018).
- <sup>83</sup>C. Barouh, T. Schuler, C.-C. Fu, and M. Nastar, "Interaction between vacancies and interstitial solutes (C, N, and O) in  $\alpha$ -Fe: From electronic structure to thermodynamics," *Phys. Rev. B* **90**, 054112 (2014).
- <sup>84</sup>G. Martin, "Phase stability under irradiation: Ballistic effects," *Phys. Rev. B* **30**, 1424–1436 (1984).
- <sup>85</sup>J.-M. Roussel and P. Bellon, "Self-diffusion and solute diffusion in alloys under irradiation: Influence of ballistic jumps," *Phys. Rev. B* **65**, 144107 (2002).
- <sup>86</sup>L. Huang, T. Schuler, and M. Nastar, "Atomic-scale modeling of the thermodynamic and kinetic properties of dilute alloys driven by forced atomic relocations," *Phys. Rev. B* **100**, 224103 (2019).
- <sup>87</sup>Y. Zhang, D. Schwen, and X.-M. Bai, "Effects of solute-SIA binding energy on defect production behaviors in Fe-based alloys," *J. Nucl. Mater.* **509**, 124–133 (2018).
- <sup>88</sup>L. Huang, K. Ma, L. Belkacemi, M. Loyer-Prost, E. Meslin, E. Toijer, L. Messina, C. Domain, J. Vidal, and M. Nastar, "Impact of the local microstructure fluctuations on radiation-induced segregation in dilute Fe-Ni and Ni-Ti model alloys: A combined modeling and experimental analysis," *Acta Mater.* **225**, 117531 (2022).
- <sup>89</sup>L. Huang, M. Nastar, L. Messina, and T. Schuler, "Elastodiffusion calculation of asymptotic absorption efficiencies and bias factors of dislocations in Al, Ni and Fe," *J. Nucl. Mater.* **570**, 153959 (2022).
- <sup>90</sup>L. Huang, "Multiscale modeling of the radiation-induced segregation in Ni-based and Fe-based dilute alloys," Ph.D. thesis (Université Paris-Saclay, 2020).
- <sup>91</sup>C. S. Becquart, N. Mousseau, and C. Domain, "L24—kinetic Monte Carlo simulations of irradiation effects," in *Comprehensive Nuclear Materials*, 2nd ed., edited by R. J. Konings and R. E. Stoller (Elsevier, Oxford, 2020), pp. 754–778.

- <sup>92</sup>F. Soisson, "Monte Carlo simulations of segregation and precipitation in alloys under irradiation," *Philos. Mag.* **85**, 489–495 (2005).
- <sup>93</sup>F. Soisson, "Kinetic Monte Carlo simulations of radiation induced segregation and precipitation," *J. Nucl. Mater.* **349**, 235–250 (2006).
- <sup>94</sup>J. Rottler, D. J. Srolovitz, and R. Car, "Kinetic Monte Carlo study of radiation-induced segregation in model metallic alloys," *Philos. Mag.* **87**, 3945–3958 (2007).
- <sup>95</sup>A. Badillo, P. Bellon, and R. S. Averback, "A phase field model for segregation and precipitation induced by irradiation in alloys," *Modell. Simul. Mater. Sci. Eng.* **23**, 035008 (2015).
- <sup>96</sup>C.-H. Huang and J. Marian, "A generalized Ising model for studying alloy evolution under irradiation and its use in kinetic Monte Carlo simulations," *J. Phys.: Condens. Matter.* **28**, 425201 (2016).
- <sup>97</sup>M. J. Lloyd, R. G. Abernethy, D. E. J. Armstrong, P. A. J. Bagot, M. P. Moody, E. Martinez, and D. Nguyen-Manh, "Radiation-induced segregation in W-Re: From kinetic monte carlo simulations to atom probe tomography experiments," *Eur. Phys. J. B* **92**, 241 (2019).
- <sup>98</sup>E. Martínez, F. Soisson, and M. Nastar, "Point defect evolution under irradiation: Finite size effects and spatio-temporal correlations," *J. Nucl. Mater.* **539**, 152233 (2020).
- <sup>99</sup>C. Becquart and F. Soisson, "Monte Carlo simulations of precipitation under irradiation," in *Handbook of Mechanics of Materials*, edited by C.-H. Hsueh (Springer Nature Singapore Pte Ltd., 2018), pp. 1–29.
- <sup>100</sup>P. C. Millett and M. Tonks, "Application of phase-field modeling to irradiation effects in materials," *Curr. Opin. Solid State Mater. Sci.* **15**, 125–133 (2011).
- <sup>101</sup>Y. Li, S. Hu, X. Sun, and M. Stan, "A review: Applications of the phase field method in predicting microstructure and property evolution of irradiated nuclear materials," *npj Comput. Mater.* **3**, 16 (2017).
- <sup>102</sup>P. Bellon and L. Thuinet, "1.25 - phase field methods," in *Comprehensive Nuclear Materials (Second Edition)*, 2nd ed., edited by R. J. Konings and R. E. Stoller (Elsevier, Oxford, 2020), pp. 779–813.
- <sup>103</sup>J. Piochaud, M. Nastar, F. Soisson, L. Thuinet, and A. Legris, "Atomic-based phase-field method for the modeling of radiation induced segregation in Fe–Cr," *Comput. Mater. Sci.* **122**, 249–262 (2016).
- <sup>104</sup>L. Thuinet, M. Nastar, E. Martinez, G. Bouobda Moladje, A. Legris, and F. Soisson, "Multiscale modeling of radiation induced segregation in iron based alloys," *Comput. Mater. Sci.* **149**, 324–335 (2018).
- <sup>105</sup>G. B. Moladje, L. Thuinet, C. Becquart, and A. Legris, "Radiation induced segregation near dislocations and symmetric tilt grain boundaries in Fe–Cr alloys: A phase-field study," *Acta Mater.* **225**, 117523 (2022).
- <sup>106</sup>Q. Bronchart, Y. Le Bouar, and A. Finel, "New coarse-grained derivation of a phase field model for precipitation," *Phys. Rev. Lett.* **100**, 015702 (2008).
- <sup>107</sup>T. Garnier, A. Finel, Y. Le Bouar, and M. Nastar, "Simulation of alloy thermodynamics: From an atomic to a mesoscale Hamiltonian," *Phys. Rev. B* **86**, 054103 (2012).
- <sup>108</sup>T. Heo and L.-Q. Chen, "Phase-field modeling of nucleation in solid-state phase transformations," *JOM* **66**, 1520–1528 (2014).
- <sup>109</sup>J.-H. Ke, E. R. Reese, E. A. Marquis, G. R. Odette, and D. Morgan, "Flux effects in precipitation under irradiation—simulation of Fe–Cr alloys," *Acta Mater.* **164**, 586–601 (2019).
- <sup>110</sup>H. Rauh and D. Simon, "On the diffusion process of point defects in the stress field of edge dislocations," *Phys. Status Solidi A* **46**, 499–510 (1978).
- <sup>111</sup>J. P. Wharry, Z. Jiao, and G. S. Was, "Application of the inverse kirkendall model of radiation-induced segregation to ferritic–martensitic alloys," *J. Nucl. Mater.* **425**, 117–124 (2012).
- <sup>112</sup>Z. Lu, R. Faulkner, G. Was, and B. Wirth, "Irradiation-induced grain boundary chromium microchemistry in high alloy ferritic steels," *Scr. Mater.* **58**, 878–881 (2008).
- <sup>113</sup>F. Soisson and T. Jourdan, "Radiation-accelerated precipitation in Fe–Cr alloys," *Acta Mater.* **103**, 870–881 (2016).
- <sup>114</sup>M. Bachhav, G. Odette, and E. Marquis, "Microstructural changes in a neutron-irradiated Fe–15 at.%Cr alloy," *J. Nucl. Mater.* **454**, 381–386 (2014).
- <sup>115</sup>M. Nastar, "Atomic diffusion theory challenging the Cahn–Hilliard method," *Phys. Rev. B* **90**, 144101 (2014).
- <sup>116</sup>J. Balbuena, L. Malerba, N. Castin, G. Bonny, and M. Caturla, "An object kinetic Monte Carlo method to model precipitation and segregation in alloys under irradiation," *J. Nucl. Mater.* **557**, 153236 (2021).
- <sup>117</sup>S. J. Rothman, L. J. Nowicki, and G. E. Murch, "Self-diffusion in austenitic Fe–Cr–Ni alloys," *J. Phys. F: Met. Phys.* **10**, 383–398 (1980).
- <sup>118</sup>J.-B. Piochaud, "Modelling of radiation induced segregation in austenitic Fe alloys at the atomistic level," Ph.D. thesis (Univeristé de Lille 1, 2013).
- <sup>119</sup>A. A. Rezwani, D. Schwen, and Y. Zhang, "Effect of concurrent grain growth on radiation-induced segregation in nanocrystalline Fe–Cr–Ni alloys," *J. Nucl. Mater.* **563**, 153614 (2022).
- <sup>120</sup>T. Allen, L. Tan, G. Was, and E. Kenik, "Thermal and radiation-induced segregation in model Ni-base alloys," *J. Nucl. Mater.* **361**, 174–183 (2007).
- <sup>121</sup>L. Barnard, J. Tucker, S. Choudhury, T. Allen, and D. Morgan, "Modeling radiation induced segregation in Ni–Cr model alloys from first principles," *J. Nucl. Mater.* **425**, 8–15 (2012).
- <sup>122</sup>M. J. Lloyd, E. Martinez, L. Messina, and D. Nguyen-Manh, "Development of a solute and defect concentration dependant Ising model for the study of transmutation induced segregation in neutron irradiated W-(Re, Os) systems," *J. Phys.: Condens. Matter.* **33**, 475902 (2021).
- <sup>123</sup>X.-M. Bai, A. F. Voter, R. G. Hoagland, M. Nastasi, and B. P. Uberuaga, "Efficient annealing of radiation damage near grain boundaries via interstitial emission," *Science* **327**, 1631–1634 (2010).
- <sup>124</sup>M. Nastar, L. T. Belkacemi, E. Meslin, and M. Loyer-Prost, "Thermodynamic model for lattice point defect-mediated semi-coherent precipitation in alloys," *Commun. Mater.* **2**, 32 (2021).
- <sup>125</sup>W. Wolfer, "Drift forces on vacancies and interstitials in alloys with radiation-induced segregation," *J. Nucl. Mater.* **114**, 292–304 (1983).
- <sup>126</sup>M. Nastar and F. Soisson, "Atomistic modeling of phase transformations: Point-defect concentrations and the time-scale problem," *Phys. Rev. B* **86**, 220102 (2012).
- <sup>127</sup>F. Soisson, E. Meslin, and O. Tissot, "Atomistic modeling of  $\alpha'$  precipitation in Fe–Cr alloys under charged particles and neutron irradiations: Effects of ballistic mixing and sink densities," *J. Nucl. Mater.* **508**, 583–594 (2018).
- <sup>128</sup>J.-H. Ke, H. Ke, G. R. Odette, and D. Morgan, "Cluster dynamics modeling of Mn–Ni–Si precipitates in ferritic–martensitic steel under irradiation," *J. Nucl. Mater.* **498**, 83–88 (2018).
- <sup>129</sup>Z. Jiao and G. Was, "Segregation behavior in proton- and heavy-ion-irradiated ferritic–martensitic alloys," *Acta Mater.* **59**, 4467–4481 (2011).
- <sup>130</sup>T. Schuler, P. Bellon, D. R. Trinkler, and R. S. Averback, "Modeling the long-term evolution of dilute solid solutions in the presence of vacancy fluxes," *Phys. Rev. Mater.* **2**, 073605 (2018).
- <sup>131</sup>H. Takahashi and N. Hashimoto, "Radiation-induced segregation and grain boundary migration in Fe–Cr–Ni model alloy under irradiation," *Mater. Trans. JIM* **34**, 1027–1030 (1993).
- <sup>132</sup>A. Volkov and A. Ryazanov, "The influence of grain boundary movement on radiation-induced segregation in binary alloys," *J. Nucl. Mater.* **256**, 108–113 (1998).
- <sup>133</sup>G. F. Bouobda Moladje, L. Thuinet, C. S. Becquart, and A. Legris, "A phase field model for dislocation climb under irradiation: Formalism and applications to pure bcc iron and ferritic alloys," *Int. J. Plasticity* **134**, 102810 (2020).
- <sup>134</sup>M. Nastar, "Segregation at grain boundaries: From equilibrium to irradiation induced steady states," *Philos. Mag.* **85**, 641–647 (2005).